

**F/6 20/6**

REDUCTION OF ANISOPLANATIC ERRORS. (U)

AUG 81 D W HANSON

**UNCLASSIFIED**

RADC-TR-81-122

ML

2015年10月15日

END

DATE \_\_\_\_\_

FILMED

12-8

OTIC



12

LEVEL II

**RADC-TR-81-122**

**In-House Report**

**August 1981**



AD A106689

# **REDUCTION OF ANISOPLANATIC ERRORS**

**Donald W. Hanson**

APPROVED FOR PUBLIC RELEASE; DISTRIBUTION UNLIMITED

**DTIC  
ELECTE  
NOV 3 1981  
S D  
B**

DTIC FILE COPY

**ROME AIR DEVELOPMENT CENTER  
Air Force Systems Command  
Griffiss Air Force Base, New York 13441**

81 11 03 018



This report has been reviewed by the RADC Public Affairs Office (PA) and is releasable to the National Technical Information Service (NTIS). At NTIS it will be releasable to the general public, including foreign nations.

RADC-TR-81-122 has been reviewed and is approved for publication.

APPROVED:

*Raymond P. Urtz, Jr.*

RAYMOND P. URTZ, JR.  
Chief, Strategic Surveillance Branch  
Surveillance Division

APPROVED:

*Frank J. Rehm*

FRANK J. REHM  
Technical Director  
Surveillance Division

FOR THE COMMANDER:

*John P. Huss*

JOHN P. HUSS  
Acting Chief, Plans Office

If your address has changed or if you wish to be removed from the RADC mailing list, or if the addressee is no longer employed by your organization, please notify RADC (OCSE) Griffiss AFB NY 13441. This will assist us in maintaining a current mailing list.

Do not return copies of this report unless contractual obligations or notices on a specific document requires that it be returned.





## MISSION of *Rome Air Development Center*

*RADC plans and executes research, development, test and selected acquisition programs in support of Command, Control Communications and Intelligence (C<sup>3</sup>I) activities. Technical and engineering support within areas of technical competence is provided to ESD Program Offices (POs) and other ESD elements. The principal technical mission areas are communications, electromagnetic guidance and control, surveillance of ground and aerospace objects, intelligence data collection and handling, information system technology, ionospheric propagation, solid state sciences, microwave physics and electronic reliability, maintainability and compatibility.*



UNCLASSIFIED

SECURITY CLASSIFICATION OF THIS PAGE (When Data Entered)

REPORT DOCUMENTATION PAGE		READ INSTRUCTIONS BEFORE COMPLETING FORM
1. REPORT NUMBER (14) RADC-TR-81-122	2. GOVT ACCESSION NO. AD-A206689	3. RECIPIENT'S CATALOG NUMBER
4. TITLE (and Subtitle) (6) REDUCTION OF ANISOPLANATIC ERRORS	5. TYPE OF REPORT & PERIOD COVERED In-House	
7. AUTHOR(s) (10) Donald W. Hanson	6. PERFORMING ORG. REPORT NUMBER N/A	
9. PERFORMING ORGANIZATION NAME AND ADDRESS Rome Air Development Center (OCSE) Griffiss AFB NY 13441	8. CONTRACT OR GRANT NUMBER(s) N/A (9) Technical Repts	
11. CONTROLLING OFFICE NAME AND ADDRESS Defense Advanced Research Projects Agency 1400 Wilson Blvd Arlington VA 22209	10. PROGRAM ELEMENT, PROJECT, TASK AREA & WORK UNIT NUMBERS (16) 62301E D1210005 (17) 00	
14. MONITORING AGENCY NAME & ADDRESS (if different from Controlling Office) Rome Air Development Center (OCSE) Griffiss AFB NY 13441	12. REPORT DATE (11) August 1981	
	13. NUMBER OF PAGES 82	
	15. SECURITY CLASS. (of this report) UNCLASSIFIED	
	15a. DECLASSIFICATION/DOWNGRADING SCHEDULE N/A	
16. DISTRIBUTION STATEMENT (of this Report)  Approved for public release; distribution unlimited		
17. DISTRIBUTION STATEMENT (of the abstract entered in Block 20, if different from Report)  Same		
18. SUPPLEMENTARY NOTES This in-house report was partially funded by ARPA		
19. KEY WORDS (Continue on reverse side if necessary and identify by block number) Propagation                      Anisoplanatic Optics Adaptive Estimation		
20. ABSTRACT (Continue on reverse side if necessary and identify by block number) The potential of reducing anisoplanatic errors in adaptive optical systems through the use of estimation theory is studied. Currently anisoplanatic errors place a fundamental limit on the performance of adaptive optical systems.  Due to the ill behaved nature of the random processes involved, the estimation procedure is formulated in terms of the structure and hyper-		

DD FORM 1 JAN 73 1473

EDITION OF 1 NOV 65 IS OBSOLETE

UNCLASSIFIED

SECURITY CLASSIFICATION OF THIS PAGE (When Data Entered)

309050

xlv



UNCLASSIFIED

SECURITY CLASSIFICATION OF THIS PAGE(When Data Entered)

structure functions. These functions are widely used in the literature dealing with turbulence and optical propagation through turbulence. A particular turbulence profile is chosen to evaluate the performance of the estimation procedure. A reasonable reduction in the ansioplanatic error is obtained through use of the estimation procedure. Only signals which are currently available in adaptive optical systems are required to implement the estimation procedure, no a priori knowledge is required.

UNCLASSIFIED

SECURITY CLASSIFICATION OF THIS PAGE(When Data Entered)



## ACKNOWLEDGEMENT

The author expresses his appreciation to Professor Nathan Schwartz of Syracuse University for the technical guidance and motivation provided during this research. The advice provided by Professor Schwartz was central to the successful completion of this effort.

Special recognition of the many useful and interesting conversations held with Dr. David L. Fried of the Optical Sciences Company during the course of this work is gratefully acknowledged.

Credit is also due to many co-workers at RADC who assisted the author in various ways, especially: Lt Jorge Fernandez; Lt Maureen Gaudette; Capt Doris Hamill; Ms. Gloria Malone; Ms. Susan Stone; and Mrs. Patricia Van Dresar.

Accession For	
NTIS GRA&I	<input checked="checked" type="checkbox"/>
DTIC TAB	<input type="checkbox"/>
Unannounced	<input type="checkbox"/>
Justification	
By	
Distribution/	
Availability Codes	
Dist	Avail and/or Special
A	



## CONTENTS

	Page
ACKNOWLEDGEMENT.....	i
LIST OF FIGURES.....	v
LIST OF TABLES.....	v
CHAPTER	
I.          INTRODUCTION.....	1
1.1    Background.....	1
1.2    Problem Statement.....	4
1.3    Research Objective.....	4
II.         STRUCTURE FUNCTIONS AND THE ANISOPLANATIC PROBLEM.....	6
2.1    Description of Random Processes.....	6
2.2    Historical Note.....	7
2.3    Structure Function Formulation.....	8
2.4    Turbulence Induced Phase Noise.....	10
2.5    Adaptive Optical Compensation.....	15
2.6    The Anisoplanatic Problem.....	17
III.        SOLUTION OF THE PREDICTION PROBLEM USING THE HYPERSTRUCTURE FUNCTION.....	22
3.1    Standard Estimation Theory.....	22
3.2    Optimum Linear Estimate for the Future Value of the Difference Between Two Random Variables of a Process.....	28
3.3    Optimum Linear Estimate for the Difference Between Two Random Variables of a Process Which is a Function of Two Variables.....	31
IV.         APPLICATION OF THE OPTIMUM LINEAR ESTIMATE TO THE ANISOPLANATIC PROBLEM.....	35
4.1    Optical Propagation Through Turbulence.....	35
4.2    Derivation of the Spatial-Angular Structure Function.....	38
4.3    Reduction of Anisoplanatic Error.....	43
V.          EVALUATION OF THE PERFORMANCE OF THE OPTIMUM ESTIMATOR.....	48
5.1    Magnitude of the Anisoplanatic Error.....	48
5.2    Reduction of the Anisoplanatic Error Through Use of the Optimum Linear Estimate..	53
VI.         CONCLUSIONS.....	61
6.1    Discussion of Results.....	61
6.2    System Implications.....	62
6.3    Recommendations for Future Work.....	63
APPENDIX	
A          SIMPLIFICATION OF THE HYPERSTRUCTURE FUNCTION....	64
REFERENCES.....	69
BIOGRAPHICAL DATA.....	71



## LIST OF FIGURES

FIGURE		Page
1-1	Adaptive Optical Receiving System.....	2
1-2	Adaptive Optical Transmitting System.....	3
1-3	Concept of Isoplanatism.....	5
2-1	Co-Located Receiver & Reference System.....	18
2-2	System With Separated Receiver & Beacon.....	20
4-1	Illustration of Anisoplanatic Phase Error.....	40
5-1	Model Turbulence Profile.....	49
5-2	Performance of the Optimum Linear Estimate for $n = 2$ .....	55
5-3	Performance of the Optimum Linear Estimate for $n = 2$ .....	56
5-4	Performance of the Optimum Linear Estimate for $n = 3$ .....	58
5-5	Performance of the Optimum Linear Estimate.....	60

## LIST OF TABLES

TABLE		Page
5-1	Values of the Integral $I_1(z, \alpha)$ .....	50
5-2	Mean Square Error.....	59



## I INTRODUCTION

### 1.1 Background

Newton observed that the atmosphere distorted the images he observed while viewing through a telescope<sup>1</sup>. Currently new systems, called adaptive optical systems, are under development to reduce the degrading effects noted by Newton<sup>2</sup>. A typical imaging adaptive optical system is shown in figure 1-1. The wavefront sensor measures the aberrations induced by the atmosphere and controls the wavefront corrector in a manner to reduce these aberrations. Adaptive optical systems are also under development for laser communications systems which transmit through the atmosphere. One particular system of interest is a ground-to-near space optical communications link. Adaptive optics is required in such a system to maintain the gain of the transmitting aperture to near its diffraction limited value. A typical transmitting adaptive optical system is shown in figure 1-2. The wavefront sensor measures the aberrations of an optical beacon signal originating at the spaceborne receiver. The wavefront corrector is adjusted to cancel these aberrations. These corrections are then imposed on the transmitted laser wavefront before it is propagated to the receiver. By reciprocity the transmitted signal arrives at the receiver with nearly diffraction limited parameters<sup>3</sup>.



# ADAPTIVE OPTICAL RECEIVING SYSTEM

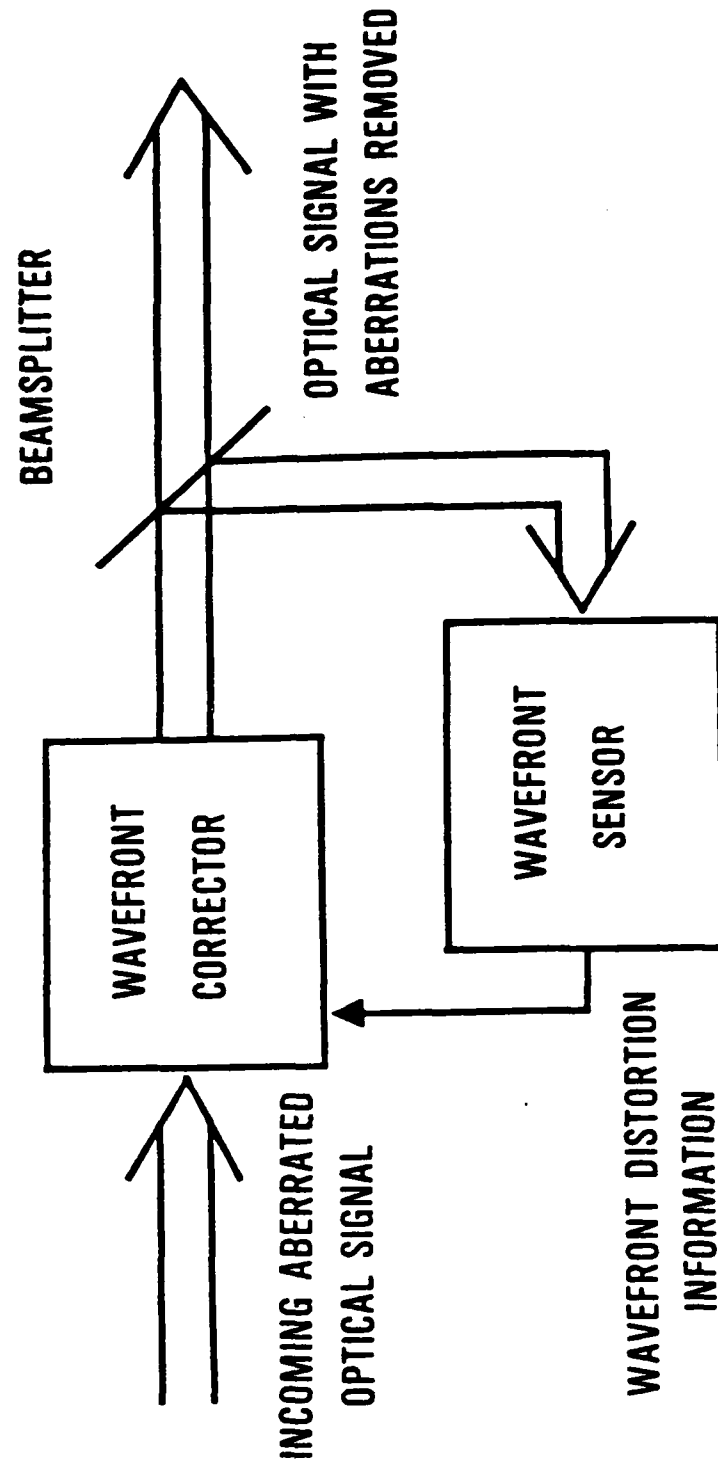


FIGURE 1-1



## ADAPTIVE OPTICAL TRANSMITTING SYSTEM

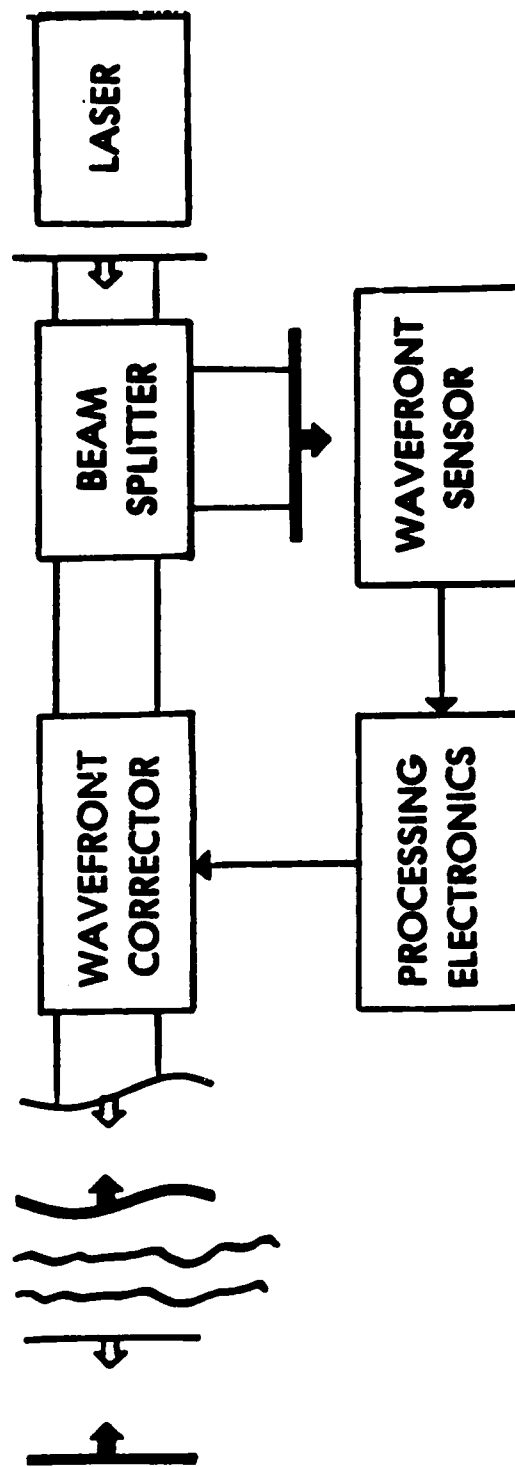


FIGURE 1-2



## 1.2 Problem Statement

A fundamental problem of both imaging and transmitting adaptive optical systems is that the degradation imposed by the atmosphere is a function of the propagation path. This concept is demonstrated in figure 1-3 in a highly exaggerated scale. The aberrations on paths 1, 2, and 3 would be nearly identical (isoplanatic)<sup>4</sup>, whereas the aberrations on paths 4 and 5 would be different (anisoplanatic). If an imaging system views an object which is large enough so that wavefronts from different portions of the object suffer different aberrations, system performance will be reduced. For a communications system transmitting to a moving receiver, time delays can cause the reference and transmitted beams to travel different paths and thus undergo different aberrations, once again reducing system performance.

## 1.3 Research Objective

The objective of this paper is to use estimation theory to reduce the degrading effects created by anisoplanatism in laser communications systems. As will be shown in the following, the application of estimation theory to this problem requires the development of new estimation procedures, since the random processes involved are not well behaved.

In the next chapter we develop the required mathematical concepts and formalize the problem statement.



## CONCEPT OF ISOPLANATISM

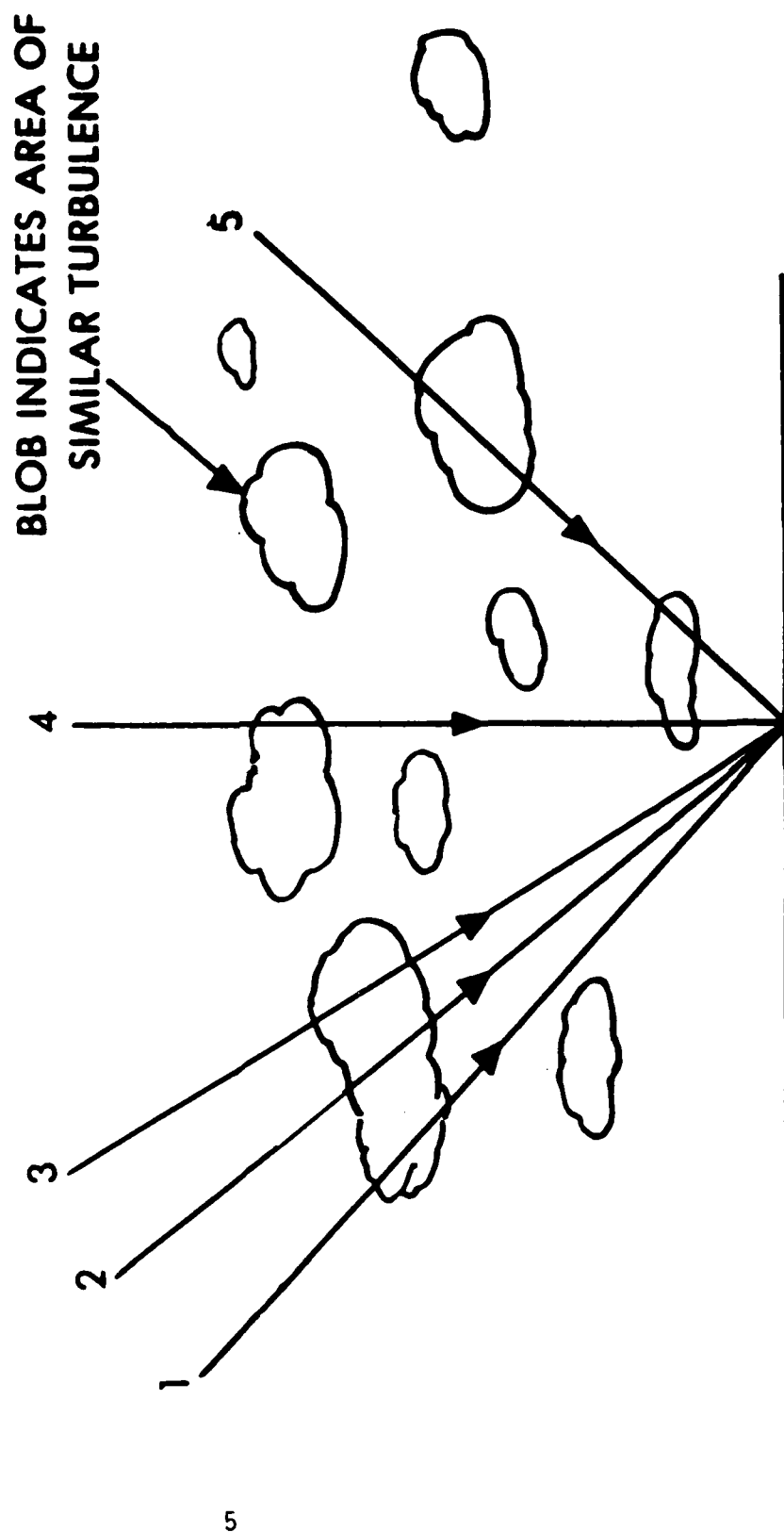


FIGURE 1-3



## II STRUCTURE FUNCTIONS AND THE ANISOPLANATIC PROBLEM

### 2.1 Description of Random Processes

In the study of real physical systems the analyses can usually be greatly simplified if the processes which describe the system can be assumed to be stationary in the wide sense (i.e., second order statistics are not a function of absolute time). However, for many physical systems of interest the assumption of wide sense stationarity cannot be used since parameters of these systems have mean values which tend to be a function of absolute time. Meteorological processes such as wind speed, temperature, and pressure are examples of processes which tend to have mean values which are a function of absolute time. Since such processes are non-stationary, they are nonergodic. Therefore, time averages cannot be used in place of ensemble averages. However, since time averages are all that are available, attempts are made to use the time averages as ensemble averages to implement the powerful statistical analysis procedures which have been developed over the last several hundred years. When attempting to use the time averages, it is difficult to assess which fluctuations are associated with first order statistics and which are associated with higher order statistics. For example, meteorological parameters such as wind speed, temperature, and pressure at a given location have variations with periods of less than 0.01 seconds and greater than days, years, and probably much



longer. Thus when using the time averages of these processes it is difficult to determine the correlation function. Large variances can result when time averages are used to approximate ensemble averages for such processes. These large variances can lead to mathematical problems when analyzing such processes.

To avoid these types of problems a statistical description, called the structure function, related to the difference between the value of the process at two different times, has been developed. The differencing process tends to suppress slow fluctuations (i.e., those which have a period longer than the differencing time) and to suppress problems associated with large variances. Time averages of the difference function are thus more representative of ensemble averages than are time averages of the basic process.

In this paper we will extend the use of the structure function to develop an optimum linear estimate of the future value of non-stationary random processes. This estimation procedure will then be applied to the problem of interest.

## 2.2 Historical Note

The concept of structure functions was first introduced by Kolmogorov<sup>5</sup>. In his work Kolmogorov used the structure function to describe the random nature of meteorological parameters. Since its introduction the structure function has been widely used in the literature to describe optical propagation through turbulence<sup>6</sup>.



Fried introduced the hyperstructure function, which is similar to the structure function, and is useful for describing processes which are a function of more than one variable<sup>7</sup>.

### 2.3 Structure Function Formulation

The temporal structure function of the random process  $f(t)$ , denoted as  $D_f(t_1, t_2)$ , is defined as follows:

$$D_f(t_1, t_2) \triangleq \langle [f(t_1) - f(t_2)]^2 \rangle \quad (2.1)$$

where the  $\langle \rangle$  brackets indicate an ensemble average.

If  $f(t)$  is non-stationary, due to non-stationarity of the mean, the structure function can be expressed in terms of  $(t_1 - t_2)$  as long as the difference function,  $h$ , defined as:

$$h(t_1, t_2) = f(t_1) - f(t_2) \quad (2.2)$$

is stationary in the mean.

We can simply show that  $h$  will be stationary in the mean provided that the mean value of the process  $f(t)$  is a linear function of  $t$ .

$$\text{Let:} \quad \langle f(t) \rangle = m + at \quad (2.3)$$

$$\text{Then:} \quad \langle h(t_1, t_2) \rangle = m + at_1 - (m + at_2) \quad (2.4)$$

$$= a(t_1 - t_2) \quad (2.5)$$



While the assumption that the mean value of a process is linear might not be completely accurate, it can be applied when the assumption of stationarity clearly cannot be used. Both theoretical and empirical data demonstrate that, for the processes that will be of interest in this paper, assuming that the structure function is not a function of absolute time is better than assuming that the process is stationary<sup>6</sup>.

We note that  $D_f$  can be written as:

$$D_f(t_1, t_2) = C_f(t_1, t_1) - 2C_f(t_1, t_2) + C_f(t_2, t_2) \quad (2.6)$$

where:  $C_f(t_1, t_2)$  is the correlation function of the process  $f$ .

For processes with large variances direct measurement of the structure function avoids the procedure of differencing large quantities, which can lead to mathematical difficulties.

The spatial structure function formulation follows in a straight forward manner from the temporal structure function. The spatial structure function of the process  $f(\vec{x})$ , denoted as  $D_f(\vec{x}_1, \vec{x}_2)$ , is defined as:

$$D_f(\vec{x}_1, \vec{x}_2) = \langle [f(\vec{x}_1) - f(\vec{x}_2)]^2 \rangle \quad (2.7)$$

The structure function depends only on the distance between  $\vec{x}_1$  and  $\vec{x}_2$  (i.e.  $|\vec{x}_1 - \vec{x}_2|$ ) if the difference function  $h(\vec{x}_1, \vec{x}_2)$  is homogenous and isotropic. As will be shown later, this assumption is realistic for the processes of interest in this paper.



The hyperstructure function,  $F$ , of the random process  $f(\vec{\gamma}, \vec{\beta})$ , where  $\vec{\gamma}$  and  $\vec{\beta}$  are two arbitrary variables (e.g., time, linear dimension, angle) is defined as:

$$F_f(\vec{\gamma}_1, \vec{\gamma}_2, \vec{\beta}_1, \vec{\beta}_2) \triangleq \langle [f(\vec{\gamma}_1, \vec{\beta}_1) - f(\vec{\gamma}_2, \vec{\beta}_1)] \times [f(\vec{\gamma}_1, \vec{\beta}_2) - f(\vec{\gamma}_2, \vec{\beta}_2)] \rangle \quad (2.8)$$

Note that for the case where  $\vec{\beta}_1 = \vec{\beta}_2$  the hyperstructure function reduces to the structure function. The purpose of the differencing procedure in equation (2.8) is to reduce the dependence of  $F$  on the absolute value of the variables  $\vec{\gamma}$  and  $\vec{\beta}$ . Thus, at least over a certain range of  $\vec{\gamma}_1 - \vec{\gamma}_2$  and  $\vec{\beta}_1 - \vec{\beta}_2$   $F$  can be written as:

$$F_f(\vec{\gamma}_1 - \vec{\gamma}_2, \vec{\beta}_1 - \vec{\beta}_2) = \langle [f(\vec{\gamma}_1, \vec{\beta}_1) - f(\vec{\gamma}_2, \vec{\beta}_1)] \times [f(\vec{\gamma}_1, \vec{\beta}_2) - f(\vec{\gamma}_2, \vec{\beta}_2)] \rangle \quad (2.9)$$

In the following sections a particular problem which can be solved using the structure function and the hyperstructure function approach will be described.

#### 2.4 Turbulence Induced Phase Noise

As stated in the introduction, the problem of interest is a ground-to-near space visible wavelength optical communications system.



The electric field of the signal, in the transmitting aperture plane, can be written as the real part of:

$$s(t', \vec{y}) = W_a(\vec{y}) A_m(t', \vec{y}) \exp\{j[\omega t' + \phi_m(t', \vec{y}) + \phi_a(t', \vec{y})]\} \quad (2.10)$$

where:  $t'$  is time in the transmitting aperture;

$\vec{y}$  is a vector denoting position in the transmitting aperture plane;

$W_a(\vec{y})$  is a function which defines the transmitting aperture;

$$W_a(\vec{y}) \triangleq \begin{cases} 1 & \text{inside the aperture} \\ 0 & \text{outside the aperture} \end{cases} \quad (2.11)$$

$A_m(t', \vec{y})$  is the amplitude modulation applied to the signal.

$\omega$  is the temporal frequency of the electromagnetic field.

$\phi_m(t', \vec{y})$  is the phase modulation applied to the signal;  
and

$\phi_a(t', \vec{y})$  is the phase imposed on the field by the transmitting antenna.

For our problem of interest the amplitude modulation and the phase modulation will be applied uniformly across the entire transmitted field, thus  $A_m$  and  $\phi_m$  will have no  $\vec{y}$  dependence.



For conventional non-adaptive systems  $\phi_a$  has no time dependence. Equation (2.10) can thus be simplified to:

$$s(t', \vec{y}) = W_a(\vec{y}) A_m(t') \exp\{j[\phi_m(t') + \phi_a(\vec{y})]\} \quad (2.12)$$

where the wt dependence is understood.

After the signal propagates through the cloud free atmosphere the received field,  $r$ , can be written as:

$$r(t, \vec{x}) = W_b(\vec{x}) A_m(t) A_p(\vec{x}) \exp\{j[\phi_p(\vec{x}) + \phi_m(t) + \phi_b(t, \vec{x}) + \gamma(t, \vec{x})]\} \quad (2.13)$$

where:  $t$  is time in the receiving aperture;

$\vec{x}$  is a vector denoting position within the receiving aperture;

$W_b(\vec{x})$  defines the size of the receiving aperture;

$\phi_b(t, \vec{x})$  is the phase imposed on the field by the receiving antenna;

$A_p(\vec{x})$  and  $\phi_p(\vec{x})$  are the amplitude and phase effects, respectively, which would result if the propagation from the transmitting plane to the receiving plane were in free space; and

$\gamma(t, \vec{x})$  is a complex random process which denotes the degradation imposed on the signal as a result of the field propagating through the turbulent atmosphere.



The terms  $A_p(\vec{x})$  and  $\phi_p(\vec{x})$  are well understood. They can be calculated using the Huygens-Fresnel integral<sup>4</sup> as follows:

$$U(t, \vec{x}) = \int_{-\infty}^{\infty} (j\lambda r)^{-1} (\exp jkr) (\cos\beta) s(t, \vec{y}) d\vec{y}; \quad (2.14)$$

$$\text{where: } U(t, \vec{x}) = A_m(t) A_p(\vec{x}) \exp j[\phi_p(\vec{x}) + \phi_m(t)]; \quad (2.15)$$

$\vec{r}$  is the vector from  $\vec{y}$  to  $\vec{x}$  and  $r$  is  $|\vec{r}|$ ;

$\beta$  is the angle between  $\vec{n}$ , the normal to the  $y$  plane, and  $\vec{r}$ ; and

$k$  is the wave number  $= 2\pi/\lambda$ .

We can separate both  $\phi_p(\vec{x})$  and  $A_p(\vec{x})$  into two parts as shown below:

$$\phi_p(\vec{x}) = \phi_p + \phi_p^1(\vec{x}) \quad (2.16)$$

$$A_p(\vec{x}) = A_p + A_p^1(\vec{x}) \quad (2.17)$$

where:  $\phi_p$  and  $A_p$  are constants.

For most applications the size of the receiving aperture, defined by  $W_b(\vec{x})$ , is chosen so that  $\phi_p^1(\vec{x})$  and  $A_p^1(\vec{x})$  do not have significant variations over the receiving aperture. Thus we can rewrite equation (2.13) as follows:

$$r(t, \vec{x}) = W_b(\vec{x}) A(t) \exp\{j[\phi_p + \phi_m(t) + \phi_b(t, \vec{x}) + \gamma(t, \vec{x})]\} \quad (2.18)$$



$$\text{where: } A(t) = A_m(t)A_p \quad (2.19)$$

We can write  $\gamma(t, \vec{x})$  as follows:

$$\gamma(t, \vec{x}) = \phi_n(t, \vec{x}) + jB(t, \vec{x}) \quad (2.20)$$

where both  $\phi_n$  and  $B$  are Gaussian random processes. Both  $\phi_n$  and  $B$  are noise-like terms which are the result of the field propagating through the turbulent atmosphere where the index of refraction,  $n$ , has a spatial dependence. It is well known that the temperature fluctuations of air are the main contributor to fluctuations in the refractive index at optical frequencies<sup>8</sup>.

Using equation (2.20) in equation (2.18) gives:

$$r(t, \vec{x}) = W_b(\vec{x})A_n(t, \vec{x})A(t)\exp\{j[\phi_p + \phi_m(t) + \phi_b(t, \vec{x}) + \phi'_n(t, \vec{x})]\} \quad (2.21)$$

$$\text{where: } A_n(t, \vec{x}) = \exp[-B(t, \vec{x})]. \quad (2.22)$$

From equation (2.21) we see that the turbulent propagation medium has induced both phase and amplitude noise on the received field. For most laser communication systems the amplitude noise does not significantly reduce system performance. The phase noise, however, does seriously degrade system performance. Fried has shown that the additive phase noise can be analyzed as limiting the effective transmitter aperture size<sup>9</sup>. The effective limit is the coherence length of the phase aberrations in the received field. This phase coherence length is denoted as  $r_0$ . The resolution



achievable when imaging through the atmosphere is also limited to that corresponding to an aperture diameter of approximately  $r_0^{10}$ .

Measurements indicate that typical nighttime values of  $r_0$  are approximately  $10 \text{ cm}^{11}$ . Using the standard definition of theoretical (i.e., diffraction limited) antenna power gain<sup>12</sup>,  $G_{DL}$ , we calculate:

$$G_{DL} = (\pi D / \lambda)^2 \quad (2.23)$$

as the gain of an aperture of diameter  $D$  at wavelength  $\lambda$ .

If the effective aperture is limited to  $r_0$  then the effective gain,  $G_e$ , is:

$$G_e = (\pi r_0 / \lambda)^2 \quad (2.24)$$

The loss due to turbulence is thus:

$$\text{Loss in gain} = (r_0 / D)^{-2} \quad (2.25)$$

For a 2 meter aperture and an  $r_0 = .1 \text{ m}$  the loss is:

$$\text{Loss in gain} = 400 \quad (2.26)$$

$$= 26 \text{ dB} \quad (2.27)$$

To recover such losses adaptive optical systems have been proposed.

## 2.5 Adaptive Optical Compensation

Adaptive optical systems adjust  $\phi_b(t, \vec{x})$  to cancel the additive phase noise,  $\phi_n(t, \vec{x})$ . The required correction is determined by measuring the phase difference between points in the receiving plane rather than the absolute phase. Using equation (2.21) the phase



difference between two points in the receiving plane is:

$$\begin{aligned}\phi(t, \vec{x}_1) - \phi(t, \vec{x}_2) &= \phi_b(t, \vec{x}_1) - \phi_b(t, \vec{x}_2) \\ &+ [\phi_n(t, \vec{x}_1) - \phi_n(t, \vec{x}_2)]\end{aligned}\quad (2.28)$$

Both the absolute phases,  $\phi_p$ , and the phase modulation,  $\phi_m$ , are suppressed by the differencing operation. Since  $\phi_p$  is not an aberration, but is merely due to a time delay and since  $\phi_m$  is a desired signal which we don't wish to modify, setting:

$$\phi_b(\vec{x}_1) - \phi_b(\vec{x}_2) = -[\phi_n(t, \vec{x}_1) - \phi_n(t, \vec{x}_2)]\quad (2.29)$$

will provide the desired compensation.

For a receiving adaptive optical system, as shown in figure 1-1, the phase noise on the incoming field is measured and the negative of the phase noise is added to the field before signal detection. For transmitting adaptive optical systems, as shown in figure 1-2, the phase noise on the field of a reference beam propagating from the receiver to the transmitter is measured. The negative of the measured phase noise is added to the outgoing field. Assuming that the reference and the transmitted beams propagate through the same turbulence, then by reciprocity the transmitted beam will arrive at the receiver without any phase noise.

Transmitting adaptive optical systems are appropriate for a ground-to-space communication link where the complexity of such systems is acceptable at the ground transmitter, but would not be in the satellite receiver.



## 2.6 The Anisoplanatic Problem

For a ground-to-space communication link in which the reference beacon and the receiver are co-located the two way propagation time between the receiver and transmitter causes the path followed by the reference beam to differ from that of the transmitted beam as shown in figure 2-1. The point ahead angle,  $\theta$ , between the propagation paths of the reference beam and the transmitted beam is:

$$\theta = 2V/c \quad (2.30)$$

where:  $V$  is the linear velocity of the satellite perpendicular to the line of sight; and  $c$  is the speed of light.

Since, as discussed in the introduction, the phase distortion imposed by the atmosphere is a function of the propagation path, the phase noise imposed on the reference beam will be different than the phase noise imposed on the outgoing transmitted beam. Thus if the phase noise on the reference beam is used to determine the phase compensation for the transmitted beam, an error is made. Such errors are called anisoplanatic errors.

There are several sources of error in adaptive optical systems such as spatial sampling errors in the wavefront sensor and the wavefront corrector, photon error in measuring the aberrated wavefront, time delay errors, amplitude scintillation errors, and anisoplanatic errors<sup>13</sup>. New methods of implementing the adaptive optics correction<sup>14</sup>, currently in the basic research stage, theoretically can reduce all of



# CO-LOCATED RECEIVER & REFERENCE SYSTEM

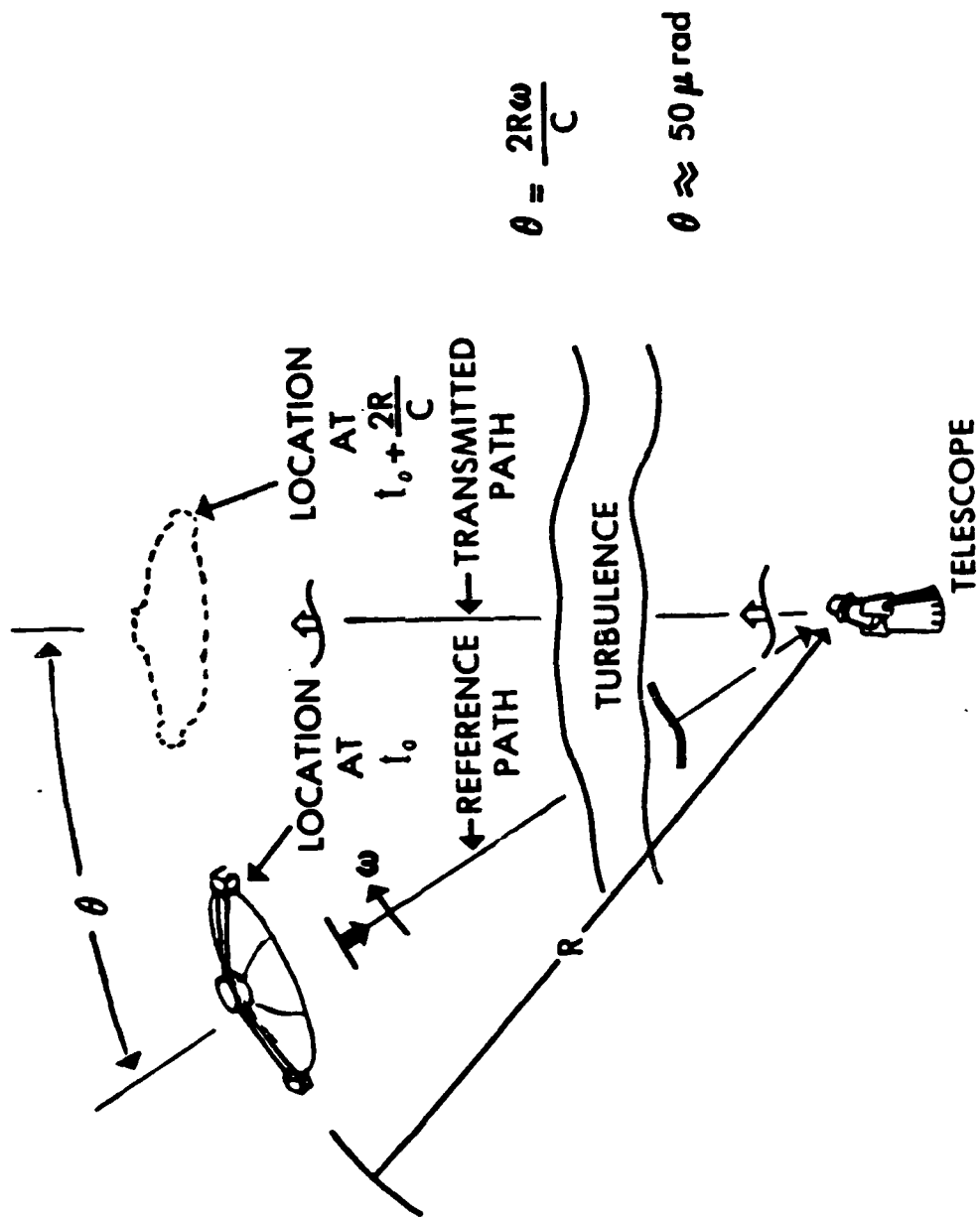


FIGURE 2-1



these errors to zero, for a system with a bright reference signal, except for the error created by anisoplanatism. Thus anisoplanatic errors currently place a fundamental limit, which is known to be severe, on the performance of the type of adaptive optical communications systems shown in figure 2-1.

To overcome the anisoplanatic errors, systems have been proposed which use a beacon in front of the receiver as shown in figure 2-2. If the angle between the beacon and the receiver, as viewed from the ground, can be kept at the point ahead angle then the anisoplanatic error can be reduced to zero. In practice, however, it is impossible to keep the beacon to receiver spacing correct at all times. This is especially true for the near earth orbiting satellites of interest since the orbital parameters are constantly changing due to atmospheric drag. The station keeping requirements (i.e., the allowable deviation in the distance between the receiver and the beacon from its correct value) are established during system design by specifying the maximum allowable anisoplanatic error. As shown later these station keeping requirements are extremely stringent. These severe station keeping requirements greatly increase the cost and complexity of the beacon and bring into question the feasibility of using a system as shown in figure 2-2.

The purpose of this paper is to investigate methods for relaxing these station keeping requirements by estimating the aberrations on one path from observing the aberrations on other paths. Thus the mathematical problem of interest is to estimate the value of a







non-stationary random process (i.e., the phase difference between two points in the aperture plane) at an unobserved point (i.e., the point ahead angle) from observed data (i.e., phase difference data at observed zenith angles). While solutions to the prediction problem are well known for stationary processes for which the correlation function is known, they must be modified for non-stationary processes. We will use the structure function and the hyperstructure function to develop an optimum linear estimate for non-stationary random processes for which the correlation function is unknown.



### III SOLUTION OF THE PREDICTION PROBLEM USING THE HYPERSTRUCTURE FUNCTION

#### 3.1 Standard Estimation Procedures

It is well known that the future value of certain random processes can be predicted exactly, in the mean square error sense<sup>15</sup>. The optimum mean square error estimate of  $f(t+\Delta t)$ , denoted as  $\hat{f}(t+\Delta t)$ , of the random process  $f(t)$  is found as follows:

$$\hat{f}(t+\Delta t) = \sum_{n=0}^{\infty} [f^{(n)}(t) (\Delta t)^n] / n! \quad (3.1)$$

where  $f^{(n)}(t)$  is the  $n$ th derivative of  $f$  with respect to  $t$ .

However, the estimation procedure provided by equation 3.1 requires that the process be stationary. We desire an estimation procedure for non-stationary processes. In practice application of equation (3.1) is difficult, even when the process is stationary, since small amounts of noise can significantly alter the higher derivatives.

The Wiener-Hopf approach to solving the prediction problem is developed as follows<sup>16</sup>. Let  $\hat{f}(t+\Delta t)$  be the estimate of  $f(t+\Delta t)$ . The estimate is given by:

$$\hat{f}(t+\Delta t) = \int_{-\infty}^t f(\beta) h(t, \beta) d\beta \quad (3.2)$$

where:  $f(\beta)$  is the observed data; and

$h(t, \beta)$  is the impulse response of the optimum linear filter.



The orthogonality principle<sup>15</sup> requires that the error in the estimate be orthogonal to the observed data, i.e.,:

$$\langle [f(t+\Delta t) - \hat{f}(t+\Delta t)] f(\beta) \rangle = 0 \quad (3.3)$$

for all  $\beta \leq t$  since  $f(\beta)$  is the observed data. Using equation (3.2) in equation (3.3) gives:

$$\langle [f(t+\Delta t) - \int_{-\infty}^t f(\beta) h(t, \beta) d\beta] f(\epsilon) \rangle = 0 \quad \epsilon \leq t \quad (3.4)$$

Taking the expectation gives:

$$C_f(t+\Delta t, \epsilon) - \int_{-\infty}^t C_f(\beta, \epsilon) h(t, \beta) d\beta = 0 \quad \epsilon \leq t \quad (3.5)$$

At this point in the development it is usually assumed that the process is stationary. We digress to discuss the solution in that case. If the process is stationary then equation (3.5) can be written as:

$$C_f(t+\Delta t - \epsilon) - \int_{-\infty}^t C_f(\beta - \epsilon) h(t - \beta) d\beta = 0 \quad \epsilon \leq t \quad (3.6)$$

Using the following change of variables:

$$\alpha = t - \beta \quad (3.7)$$

in equation (3.6) gives:

$$C_f(t+\Delta t - \epsilon) - \int_0^{\infty} C_f(t - \alpha - \epsilon) h(\alpha) d\alpha = 0 \quad \epsilon \leq t \quad (3.8)$$



Using another change of variables:

$$t - \epsilon = \tau \quad (3.9)$$

in equation (3.8) gives:

$$C_f(\tau + \Delta t) - \int_0^{\infty} C_f(\tau - \alpha) h(\alpha) d\alpha = 0 \quad (3.10)$$

which is true for all  $\tau \geq 0$ . This is the standard form of the Wiener-Hopf integral equation. Procedures have been developed for solving this equation<sup>16</sup>.

From a practical point of view the Wiener-Hopf approach has two drawbacks. First it requires complete knowledge of the correlation function  $C_f(t_1, t_2)$  for all times  $t_1$  and  $t_2$ . Complete specification of  $C_f$  is not available for many practical problems. Secondly, standard solutions are known only for the case where the process is stationary. Trying to apply known procedures for solving equation (3.10) to solve equation (3.5) would be tedious. Such a solution would obviously require that the impulse response,  $h$ , be time varying.

To avoid the requirement of knowing  $C_f(t_1, t_2)$  for all times  $t_1, t_2$  we can use an estimation procedure based on discrete time samples of the observed data. The standard approach for the optimum estimate in this case is developed as follows. We assume that we have the observed data set  $\{f_i\}$  where:

$$f_i = f(t_i) \quad (3.11)$$



We represent the observed data as a vector  $\vec{f}$  where:

$$\vec{f} = \begin{bmatrix} f_1 \\ f_2 \\ \cdot \\ \cdot \\ f_n \end{bmatrix} \quad (3.12)$$

We wish to form an estimate of  $f(t+\Delta t)$  which we denote as  $\hat{f}(t+\Delta t)$ . The optimum linear estimate is given by:

$$\hat{f}(t+\Delta t) = \vec{a} \cdot \vec{f} \quad (3.13)$$

where: the vector multiplication is the standard inner product;  
the vector  $\vec{a}$  is chosen such that the orthogonality principle  
is satisfied, i.e.,:

$$\langle [f(t+\Delta t) - \hat{f}(t+\Delta t)] \vec{f} \rangle = 0 \quad (3.14)$$

Using equation (3.13) in equation (3.14) gives:

$$\langle [f(t+\Delta t) - \vec{a} \cdot \vec{f}] \vec{f} \rangle = 0 \quad (3.15)$$

Carrying out the multiplications and the expectation gives the matrix equation.



$$\begin{bmatrix}
 C_f(t+\Delta t, t_1) - \{a_1 C_f(t_1, t_1) + a_2 C_f(t_2, t_1) + \dots + a_n C_f(t_n, t_1)\} \\
 C_f(t+\Delta t, t_2) - \{a_1 C_f(t_1, t_2) + a_2 C_f(t_2, t_2) + \dots + a_n C_f(t_n, t_2)\} \\
 \vdots \\
 C_f(t+\Delta t, t_n) - \{a_1 C_f(t_1, t_n) + a_2 C_f(t_2, t_n) + \dots + a_n C_f(t_n, t_n)\}
 \end{bmatrix}$$

$$= \vec{0} \quad (3.16)$$



Solution of this equation determines the vector  $\vec{a}$  which will provide the optimum linear estimate. If the process is stationary equation (3.16) can be written as follows:

$$\begin{bmatrix}
 C_f(t+\Delta t-t_1) - \{ a_1 C_f(0) + a_2 C_f(t_2-t_1) + \dots + a_n C_f(t_n-t_1) \} \\
 C_f(t+\Delta t-t_2) - \{ a_1 C_f(t_1-t_2) + a_2 C_f(0) + \dots + a_n C_f(t_n-t_2) \} \\
 \cdot \\
 \cdot \\
 \cdot \\
 C_f(t+\Delta t-t_n) - \{ a_1 C_f(t_1-t_n) + a_2 C_f(t_2-t_n) + \dots + a_n C_f(0) \}
 \end{bmatrix}
 = \vec{0} \quad (3.17)$$



Both equations (3.16) and (3.17) require knowledge of the correlation function. We also note that equations (3.16) and (3.17) involve the difference of the variance and the correlation function of the process for various times. Thus for processes with large variances, equations (3.16) and (3.17) pose a mathematical stability problem, since they involve the difference of large quantities in an attempt to observe small quantities.

### 3.2 Optimum Linear Estimate for the Future Value of the Difference Between Two Random Variables of a Process

For many practical cases of interest the value of a process at some absolute time is not what is required. Many times the problem can instead be formulated such that it is the difference between the value of the random process at two different times that is of interest. Formulation of the problem in such a manner allows use of the hyperstructure function and the structure function, functions which can be observed, to describe the process. We now develop the optimum linear estimate for the future value of the difference between two random variables of the same process.

We desire an estimate,  $\hat{h}(t+\Delta t)$ , of  $h(t+\Delta t)$  where:

$$h(t+\Delta t) = f(t) - f(t+\Delta t) \quad (3.18)$$

For many processes the differencing procedure in equation (3.18) will remove the non-stationary aspects of the process  $f(t)$ , at least for a certain range of  $\Delta t$ . For processes for which this is true, such as meteorological processes<sup>6</sup>, we can use time averages to approximate ensemble averages.



Obviously one approach to forming the desired estimate would be to measure  $f(t)$  and to form an estimate of  $f(t+\Delta t)$  separately using the procedures discussed in section 3.1. We develop another approach which does not require the assumption of stationarity or knowledge of the correlation function of the process.

We will use the observed data set  $\{h_i\}$  where:

$$h_i(\Delta t) = f(t_i) - f(t_i + \Delta t) \quad (3.19)$$

We define the temporal hyperstructure function for a process, which is a function of a single variable, as follows:

$$F_f(t_i - t_j, \Delta t) \triangleq \langle [h_i(\Delta t)][h_j(\Delta t)] \rangle \quad (3.20)$$

We note that for  $t_i = t_j$  the temporal hyperstructure function reduces to the temporal structure function. We form a linear estimate of  $h(t+\Delta t)$  as follows:

$$\hat{h}(t+\Delta t) = \vec{a} \cdot \vec{h} \quad (3.21)$$

and optimize the estimate by requiring that:

$$\langle [h(t+\Delta t) - \vec{a} \cdot \vec{h}] \vec{h} \rangle = \vec{0} \quad (3.22)$$

Multiplying and taking the expectation gives:



$$\begin{bmatrix}
 F_f(t-t_1, \Delta t) - [a_1 D_f(\Delta t) + a_2 F_f(t_2-t_1, \Delta t) + \dots + a_n F_f(t_n-t_1, \Delta t)] \\
 F_f(t-t_2, \Delta t) - [a_1 F_f(t_1-t_2, \Delta t) + a_2 D_f(\Delta t) + \dots + a_n F_f(t_n-t_2, \Delta t)] \\
 \cdot \quad \cdot \quad \cdot \quad \cdot \quad \cdot \\
 \cdot \quad \cdot \quad \cdot \quad \cdot \quad \cdot \\
 \cdot \quad \cdot \quad \cdot \quad \cdot \quad \cdot \\
 F_f(t-t_n, \Delta t) - [a_1 F_f(t_1-t_n, \Delta t) + a_2 F_f(t_2-t_n, \Delta t) + \dots + a_n D_f(\Delta t)]
 \end{bmatrix}$$

$$= \vec{0} \quad (3.23)$$

where  $D_f(\Delta t)$  is the temporal structure function of the process  $f(t)$ .



Comparing equations (3.23) and (3.17) we see that they are identical except that in equation (3.23) the hyperstructure function,  $F$ , and the structure function,  $D$ , have replaced the correlation function,  $C$ . It is important to emphasize that  $F$  and  $D$  can be determined through time domain averages since the differencing procedure creates a process which is stationary, at least for some values of  $\Delta t$ . Thus equation (3.23) can be solved since the  $F_f(t_i - t_j, \Delta t)$  and  $D_f(\Delta t)$  can be determined, whereas neither equation (3.16) nor equation (3.17) can be solved since the  $C_f$ 's cannot be determined through time domain averages<sup>17</sup>. Also the problems associated with large variances have been suppressed through the use of the hyperstructure function since equation (3.23) involves the difference of small quantities while attempting to observe small quantities.

### 3.3 Optimum Linear Estimate for the Difference Between Two Random Variables of a Process Which is a Function of Two Variables

The development in this section follows that in the previous section very closely. Here the problem of interest is to predict the future value of the difference between two random variables of a process which is a function of both space and time.

We desire to form an estimate,  $\hat{g}(\rho, t + \Delta t)$ , of  $g(\rho, t + \Delta t)$  where:

$$g(\rho, t) = [f(\vec{x}_1, t) - f(\vec{x}_2, t)] \quad (3.24)$$

$$\text{and } \rho = |x_1 - x_2| \quad (3.25)$$



We note that implicit in the definition of equation (3.24) is the assumption that the differencing procedure has removed any non-homogeneous and non-isotropic characteristics of the process  $f(t)$ , thus making  $g$  a function of  $\rho$  and  $t$  only.

Obviously one approach to forming the desired estimate would be to form an estimate of  $f(\vec{x}_1, t+\Delta t)$  and  $f(\vec{x}_2, t+\Delta t)$  separately using the procedures discussed in section 3.1. As before, we develop another approach which does not require the assumption of stationarity or knowledge of the correlation function of the process.

We will use the observed data set  $\{g_i(\rho)\}$  where:

$$g_i(\rho) \triangleq g(\rho, t_i) \quad (3.26)$$

Using equation (2.9) we note that:

$$\langle g_i(\rho) g_j(\rho) \rangle = F_f(\rho, t_i - t_j) \quad (3.27)$$

Implicit in equation (3.27) is the assumption that the differencing procedure has removed any non-stationary characteristics of  $f$ .

We form a linear estimate of  $g(\rho, t+\Delta t)$  as follows:

$$\hat{g}(\rho, t+\Delta t) = \vec{a} \cdot \vec{g} \quad (3.28)$$

and optimize the estimate by requiring that:

$$\langle [g(\rho, t+\Delta t) - \vec{a} \cdot \vec{g}] \vec{g} \rangle = \vec{0} \quad (3.29)$$

Multiplying and taking the expectation gives:



$$\begin{bmatrix}
 F_f(\rho, t+\Delta t-t_1) - \{ a_1 D_f(\rho) + a_2 F_f(\rho, t_2-t_1) + \dots + a_n F_f(\rho, t_n-t_1) \} \\
 F_f(\rho, t+\Delta t-t_2) - \{ a_1 F_f(\rho, t_1-t_2) + a_2 D_f(\rho) + \dots + a_n F_f(\rho, t_n-t_2) \} \\
 \cdot \quad \cdot \quad \cdot \quad \cdot \quad \cdot \\
 F_f(\rho, t+\Delta t-t_n) - \{ a_1 F_f(\rho, t_1-t_n) + a_2 F_f(\rho, t_2-t_n) + \dots + a_n D_f(\rho) \}
 \end{bmatrix}$$

$$= \vec{0} \quad (3.30)$$

where  $D_f(\rho)$  is the spatial structure function of  $f$ .



Comparing equations (3.30) and 3.17) we see that they are identical except that in equation (3.30) the hyperstructure function,  $F$ , and the structure function,  $D$ , have replaced the correlation function,  $C$ . It is important to emphasize that  $F$  and  $D$  can be determined through time domain averages since the differencing procedure creates a process which is stationary, at least for some values of  $\rho$  and  $\Delta t$ . Thus equation (3.30) can be solved since the  $F_f(\rho, t_i - t_j)$  can be determined, whereas neither equation (3.16) nor equation (3.17) can be solved since the  $C_f$ 's cannot be determined through time domain averages. Once again we note that the problems associated with having a process with large variances are suppressed in equation (3.30).



# IV APPLICATION OF THE OPTIMUM LINEAR ESTIMATE TO THE ANISOPLANATIC PROBLEM

## 4.1 Optical Propagation Through Turbulence

A great deal of research has been conducted in the area of optical propagation through the turbulent atmosphere. Numerous books and articles have resulted from this research, such as the pioneering work by Tatarski<sup>6</sup> and the more recent work by Strohbehn<sup>17</sup>. To make this paper relatively self-contained, we review the results of others which will be used later in the paper.

The spatial structure function for the index of refraction,  $D_n$ , is given by:

$$D_n(\vec{x}_1, \vec{x}_2) = \langle [n(\vec{x}_1) - n(\vec{x}_2)]^2 \rangle \quad (4.1)$$

where:  $n(\vec{x})$  is the index of refraction at  $\vec{x}$ , and;

$$n(\vec{x}) = \sqrt{e(\vec{x})} \text{ where } e(\vec{x}) \text{ is the dielectric constant at } \vec{x}.$$

It is known<sup>6</sup> that under certain conditions  $D_n$  can be written as follows:

$$D_n(\rho) = C_n^2 \rho^{2/3} \quad (4.2)$$

where:  $C_n^2$  is called the index of refraction structure parameter, and;

$$\vec{\rho} = \vec{x}_1 - \vec{x}_2, \text{ and;} \quad (4.3)$$

$$\rho = |\vec{\rho}| \quad (4.4)$$



$C_n^2$  thus provides a measure of the strength of turbulence. The range over which equation (4.2) holds is called the inertial sub-range and is given by:

$$l_0 \ll \rho \ll L_0 \quad (4.5)$$

where  $l_0$  is called the inner scale of turbulence and  $L_0$  is called the outer scale of turbulence. Physically  $l_0$  and  $L_0$  correspond to the smallest and largest size elements, respectively, in the turbulent field over which the index of refraction is constant. Turbulence which is specified by equation (4.2) is called Kolmogorov turbulence.

Starting with the assumption of Kolmogorov turbulence, the spatial structure function of phase,  $D_\phi(\rho)$ , for a plane wavefront propagating through a turbulent medium is given by<sup>6</sup>:

$$D_\phi(\rho) = 2.91 k^2 L^{5/3} \int_0^L C_n^2(v) dv \quad (4.6)$$

$$\text{where: } k = 2\pi/\lambda, \quad (4.7)$$

$\lambda$  is the wavelength of the optical field,

$L$  is the path length,

$v$  is the distance along the path from the receiver to the transmitter, and

$$(0.033) (2^{1/3}) (\pi^2) (6/5) [\Gamma(1/6)][\Gamma(11/6)]^{-1} \approx 2.91 \quad (4.8)$$

and  $\Gamma(y)$  is the well known Gamma function<sup>18</sup>.



Equation (4.6) can be written as:

$$D_{\phi}(\rho) = A \rho^{5/3} \quad (4.9)$$

$$\text{where: } A = 2.91 k^2 \int_0^L C_n^2(v) dv \quad (4.10)$$

Fried<sup>10</sup> has defined a parameter  $r_0$  as follows:

$$r_0 \triangleq \{2[(24/5)\Gamma(6/5)]^{5/6}/A\}^{3/5} \quad (4.11)$$

$$= (6.88/A)^{3/5} \quad (4.12)$$

The physical significance of  $r_0$  as defined by equation (4.11) is that  $r_0$  can be considered to be the diffraction limit of the turbulent medium through which the optical wave is propagating. Using equation (4.12) in equation (4.9) gives:

$$D_{\phi}(\rho) = 6.88 (\rho/r_0)^{5/3} \quad \text{rad}^2 \quad (4.13)$$

We can find  $r_0$  from the parameters of the path by using equation (4.11) in equation (4.10) to get:

$$r_0 = [0.423 k^2 \int_0^L C_n^2(v) dv]^{-3/5} \quad (4.14)$$

We note that the integral in equation (4.14) is unweighted, therefore,  $r_0$  for a plane wave is not a function of where the turbulence is along the propagation path. Thus,  $r_0$  is the same for both ground to space and space to ground plane wave propagation.



Finally, we note that  $C_n^2$  is most often known as a function of altitude,  $h$ , above ground. We thus rewrite equation (4.14) for ground to space plane wave propagation as:

$$r_0 = [0.423 k^2 (\sec \psi) \int_0^\infty C_n^2(h) dh]^{-3/5} \quad (4.15)$$

where:  $\psi$  = zenith angle;

$$v = h/\cos\psi, \text{ and;} \quad (4.16)$$

the upper limit of integration is determined by the altitude where atmospheric turbulence ends (i.e.,  $C_n^2$  goes to zero), which is approximately 20km<sup>19</sup>.

If  $r_0$  is known, we can use equation (4.13) to determine the mean square phase difference between points in the aperture plane, for a given zenith angle.

#### 4.2 Derivation of the Spatial-Angular Structure Function

Others have previously calculated the anisoplanatic error<sup>20, 21</sup>. We follow a slightly different development which concisely states the anisoplanatic error in terms of a single structure function.

We define the spatial-angular structure function, denoted as  $H_\phi(\vec{\rho}, \vec{\theta})$ , as follows:

$$H_\phi(\vec{\rho}, \vec{\theta}) = \langle \{ [\phi(\vec{x}_1, \vec{\psi}_1) - \phi(\vec{x}_2, \vec{\psi}_1)] - [\phi(\vec{x}_1, \vec{\psi}_2) - \phi(\vec{x}_2, \vec{\psi}_2)] \}^2 \rangle \quad (4.17)$$

$$\text{where: } \vec{\theta} = \vec{\psi}_1 - \vec{\psi}_2 \quad (4.18)$$



$H_\phi(\vec{\rho}, \vec{\theta})$  is the mean square phase difference between two points in the aperture plane at two different zenith angles. Thus,  $H_\phi(\vec{\rho}, \vec{\theta})$  quantifies the anisoplanatic error. Figures 4-1a, b, and c illustrate the nomenclature used in equation (4.17). As shown in figures 4-1b and c, the phase difference between points  $\vec{x}_1$  and  $\vec{x}_2$  will in general be different for different zenith angles due to atmospheric distortion. This is what creates the anisoplanatic error.

Expanding the square in equation (4.17) gives:

$$\begin{aligned} H_\phi(\vec{\rho}, \vec{\theta}) = & \langle [\phi(\vec{x}_1, \vec{\psi}_1) - \phi(\vec{x}_2, \vec{\psi}_1)]^2 \\ & - 2\{[\phi(\vec{x}_1, \vec{\psi}_1) - \phi(\vec{x}_2, \vec{\psi}_1)][\phi(\vec{x}_1, \vec{\psi}_2) - \phi(\vec{x}_2, \vec{\psi}_2)]\} \\ & + [\phi(\vec{x}_1, \vec{\psi}_2) - \phi(\vec{x}_2, \vec{\psi}_2)]^2 \rangle \end{aligned} \quad (4.19)$$

Using equation (2.9) we can rewrite equation (4.19) as follows:

$$H_\phi(\vec{\rho}, \vec{\theta}) = 2[F_\phi(\vec{\rho}, \vec{0}) - F_\phi(\vec{\rho}, \vec{\theta})] \quad (4.20)$$

Fried<sup>22</sup> found  $F_\phi(\vec{\rho}, \vec{\theta})$  to be given by:

$$\begin{aligned} F_\phi(\vec{\rho}, \vec{\theta}) = & 8.16 k^2 (4\pi)^{-1} \int_0^L dv C_n^2(v) \int d\vec{\sigma} \{ [1 - \exp(i\vec{\sigma} \cdot \vec{\rho})] \\ & \sigma^{-11/3} [\cos(\vec{\sigma} \cdot \vec{\theta} v) + \cos(v\sigma^2/k)] \} \end{aligned} \quad (4.21)$$

where:  $\vec{\sigma}$  is two dimensional spatial frequency:

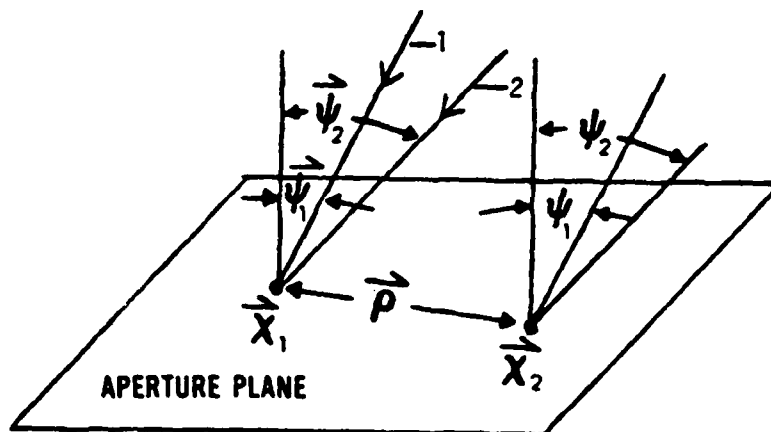
$$\sigma = |\vec{\sigma}|;$$

$$\theta = |\vec{\theta}|;$$

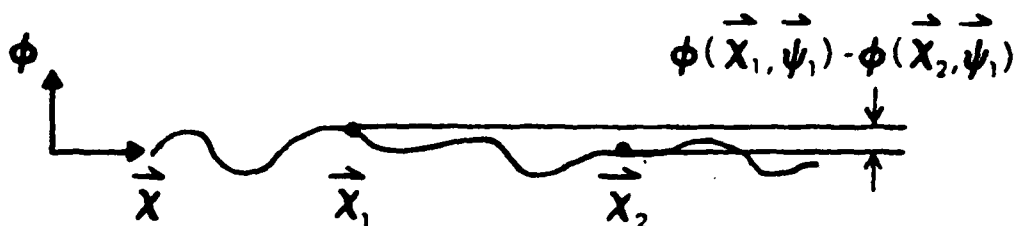


# ILLUSTRATION OF ANISOPLANATIC PHASE ERROR

- a. TWO TYPICAL POINTS IN THE APERTURE PLANE RECEIVING OPTICAL SIGNALS FROM TWO TYPICAL ZENITH ANGLES



- b. OPTICAL PHASE AS A FUNCTION OF LOCATION IN THE APERTURE PLANE FOR ZENITH ANGLE  $\vec{\psi}_1$



- c. OPTICAL PHASE AS A FUNCTION OF LOCATION IN THE APERTURE PLANE FOR ZENITH ANGLE  $\vec{\psi}_2$

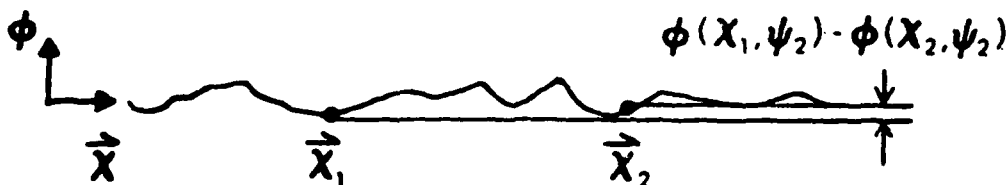


Figure 4-1



$v$  is the distance along the propagation path from receiver to transmitter, and;

$$10\pi^2 [27\pi(4/3) \sin(\pi/6)]^{-1} = 8.16 \quad (4.22)$$

Equation (4.21) is valid for the inertial sub-range as defined by equation (4.5). Using equation (4.21) in equation (4.20) gives:

$$H_{\phi}(\vec{\rho}, \vec{\theta}) = 8.16 k^2 (2\pi^2)^{-1} \int_0^L dv C_n^2(v) \int d\vec{\sigma} \sigma^{11/3} \{ [1 - \exp(i\vec{\sigma} \cdot \vec{\rho})] [1 - \cos(\vec{\sigma} \cdot \vec{\theta} v)] \} \quad (4.23)$$

In Appendix A we reduce an integral similar to the integral in equation (4.23). Following the procedure here that is used in Appendix B we find:

$$H_{\phi}(\vec{\rho}, \vec{\theta}) = 2.91 k^2 (\sec \psi) \rho^{5/3} \int_0^{\infty} dh C_n^2(h) \{ 1 + (zh)^{5/3} - (1/2) [1 + 2hz \cos \alpha + (zh)^2]^{5/6} - (1/2) [1 - 2hz \cos \alpha + (zh)^2]^{5/6} \} \quad (4.24)$$

where:  $\psi$  is the zenith angle;

$$z = (\theta \sec \psi) / \rho; \quad (4.25)$$

$h$  is the vertical distance (i.e., altitude) above the ground transmitter, and;

$\alpha$  is the angle between  $\vec{\rho}$  and  $\vec{\theta}$ .



For propagation paths originating at the same point in the aperture plane, (i.e., paths 1 and 2 in figure 4-1a) the first few meters of the paths will be spaced closer than the inner scale. For an angle of 50  $\mu$ rad the paths will be within 1 mm for 20 meters. Since this is a very small portion of the total path, the results should still be highly accurate. We note that for separations less than the inner scale the structure function is known to be proportional to  $\rho^2$ , thus the use of the  $\rho^{5/3}$  assumption overestimates the strength of turbulence<sup>6</sup>. At the top of the turbulent atmosphere the separation between the paths has increased by  $\gamma Z$  where  $Z$  is the top of the turbulent atmosphere ( $\sim 20$ km) and  $\gamma$  is the angle between propagation paths. It is believed that the outer scale,  $L_0$ , is on the order of 100 m at the top of the atmosphere<sup>23</sup>. Thus:

$$\gamma Z \ll 100 \text{ m} \quad (4.26)$$

Using  $Z = 20$ km in equation (4.26) gives:

$$\gamma \ll 5 \text{ mrad} \quad (4.27)$$

Thus the maximum separation in angle between any element of the observed data set  $\{g_i(\vec{\rho})\}$  where:

$$g_i(\vec{\rho}) = g(\vec{\rho}, \psi_i) = \phi(\vec{x}_1, \vec{\psi}_i) - \phi(\vec{x}_2, \vec{\psi}_i) \quad (4.28)$$

and  $g(\vec{\rho}, \vec{\psi} + \vec{\theta})$ , the quantity to be estimated, must be much less than 5 mrad.



Equation (4.24) is the basic result of this section. It determines the anisoplanatic error in terms of the propagation path. In general, the integral must be evaluated using numerical techniques for a particular  $C_n^2(h)$  profile. We will evaluate equation (4.24) in Chapter 5.

### 4.3 Reduction of the Anisoplanatic Error

We wish to reduce the anisoplanatic error given by H. We pause briefly to recapitulate that our knowledge of the additive phase noise is limited. What we know about the process is its structure function, equation (4.6), its hyperstructure function, equation (4.21), and its spatial-angular structure function, equation (4.24). These equations are all developed based on the assumption that the turbulence is Kolmogorov. Thus, for these equations to be valid the separation between the propagation paths in figure 4-1 must be within the inertial sub-range as defined by equation (4.5). While we don't know exactly what  $l_0$  and  $L_0$  are, we do know that in the aperture plane  $l_0$  is on the order of a millimeter and  $L_0$  is on the order of the height above ground<sup>23</sup>. For our case of interest the minimum  $\rho$  in the aperture plane will be the separation between actuators in the wavefront corrector. This separation is on the order of  $r_0$ <sup>24</sup>, which is approximately 0.1m. The maximum separation in the aperture plane is determined by the diameter of the transmitting aperture, therefore, the transmitting aperture must be higher above ground than its diameter, which is almost always the case.



Finally, the last assumption that we must make is the so called Taylor's hypothesis, also called the frozen flow theory<sup>25</sup>. This theory assumes that in the time scales of interest the elements of turbulence remain fixed in shape (i.e., "frozen"). Time variations in the turbulence induced aberrations are assumed to be caused by the wind transporting the "frozen" turbulence pattern through the propagation path.

The ambient winds along a propagation path from ground to space have varying speeds and directions as a function of altitude, thus for a system with a fixed propagation path the turbulence pattern would be moving in a random fashion and no prediction would be possible. For a near earth satellite, however, the slew rate of the line of sight (i.e.,  $\dot{\psi}$ ) will cause the propagation path to cut through the atmosphere, thus, producing a pseudo-wind. If the speed of the pseudo-wind predominates over the natural winds at all altitudes, then the turbulence pattern at each altitude will appear to move at the same angular velocity. For a satellite at an altitude of 200 km the slew rate of the line of sight is approximately 0.039 rad/sec near zenith. The tangential velocity at altitude  $h$  is thus:

$$v = (0.039) h \text{ m/sec} \quad (4.29)$$

In the lower altitudes, wind speeds are usually under 8 m/sec<sup>26</sup>. Thus for  $h > 200$  m the pseudo-wind will predominate over the ambient winds. The maximum wind speed, approximately 100 m/sec, usually occurs at about 12 km<sup>26</sup>. At 12 km, the pseudo-wind speed is 468 m/sec, thus the pseudo-wind easily predominates at the higher altitudes. Thus, there is a direct relationship between time and the angle moved at each height of turbulence, for low earth orbiting



satellites. This allows us to translate an observation over a certain time interval to an observation over a corresponding angle, and thus, allows use of equation (4.21) in equation (3.23). Therefore, the optimum linear estimate for the point ahead angle,  $\vec{\theta}$ , is given by:

$$\hat{g}(\vec{\rho}, \vec{\psi} + \vec{\theta}) = \vec{a} \cdot \vec{g} \quad (4.30)$$

where: all angles are coplanar, and;

$\vec{a}$  is determined by solving:



$$\begin{bmatrix}
 F_{\phi}(\vec{\rho}, \vec{\psi} + \vec{\theta} - \vec{\psi}_1) - \{ a_1 F_{\phi}(\vec{\rho}, \vec{0}) + a_2 F_{\phi}(\vec{\rho}, \vec{\psi}_2 - \vec{\psi}_1) + \dots + a_n F_{\phi}(\vec{\rho}, \vec{\psi}_n - \vec{\psi}_1) \} \\
 F_{\phi}(\vec{\rho}, \vec{\psi} + \vec{\theta} - \vec{\psi}_2) - \{ a_1 F_{\phi}(\vec{\rho}, \vec{\psi}_1 - \vec{\psi}_2) + a_2 F_{\phi}(\vec{\rho}, \vec{0}) + \dots + a_n F_{\phi}(\vec{\rho}, \vec{\psi}_n - \vec{\psi}_2) \} \\
 \cdot \quad \cdot \quad \cdot \\
 F_{\phi}(\vec{\rho}, \vec{\psi} + \vec{\theta} - \vec{\psi}_n) - \{ a_1 F_{\phi}(\vec{\rho}, \vec{\psi}_1 - \vec{\psi}_n) + a_2 F_{\phi}(\vec{\rho}, \vec{\psi}_2 - \vec{\psi}_n) + \dots + a_n F_{\phi}(\vec{\rho}, \vec{0}) \}
 \end{bmatrix}$$

$$= \vec{0} \quad (4.31)$$



and where:  $(\psi + \theta - \psi_i) \ll 5 \text{ mrad}$ , for all  $i$  (4.32)

according to equation (4.27).

Equations (4.30), (4.31), and (4.32) are the basic result of this section. In the next chapter we will evaluate the anisoplanatic error for a typical case and determine how much this error can be reduced through utilization of the optimum estimate. In an operating adaptive optical system the data necessary to determine the optimum estimate (i.e., the  $F_\phi$ 's) would be available. For an analytical evaluation of the performance, we will calculate the  $F_\phi$ 's using a model turbulent atmosphere.



## V. EVALUATION OF THE PERFORMANCE OF THE OPTIMUM ESTIMATOR

In this chapter we will obtain numerical results to determine how well the optimum estimator performs. First we evaluate the error without the estimate and then the error with the estimate.

### 5.1 Magnitude of the Anisoplanatic Error

The anisoplanatic error is given by equation (4.24). To evaluate the integral a profile of turbulence, i.e.,  $C_n^2$  as a function of  $h$ , must be selected. The most extensive measurements of the strength of turbulence as a function of altitude have been made at the ARPA Maui Optical Station. The model of  $C_n^2$  versus  $h$  derived from those measurements is shown in figure 5-1.<sup>27</sup> This model will be used to evaluate the performance of the optimum estimator. Once we know what to use for  $C_n^2$  in equation (4.24) we can perform a numerical integration. This numerical integration was accomplished using a computer program adapted from Fried<sup>28</sup>. Table 5-1 lists the value of the integral,  $I_1$ , as a function of the parameter  $z$  and the angle  $\alpha$ .

For a typical case of  $\rho = 1$  m;  $\psi = 0$ ;  $\alpha = 0$ ; and a point ahead angle,  $\theta = 50$   $\mu$ rad; using table 5-1 and equation (4.24) we see that:



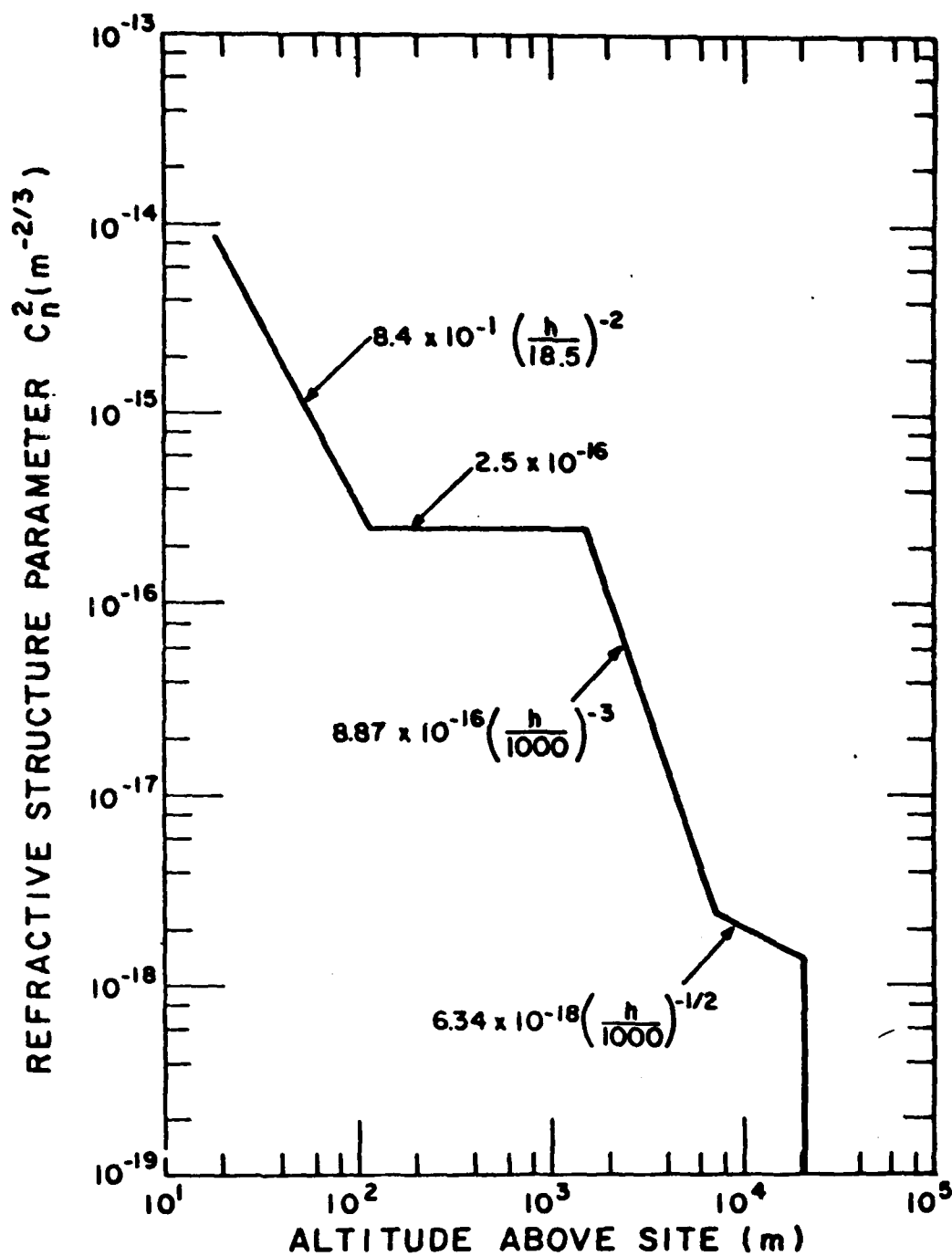


FIGURE 5-1



# VALUES OF INTEGRAL $I_1(z, \alpha)$

z	ANGLE $\alpha$			
	0.0	45.0	60.0	75.0
1.00e+00	5.798e-13	5.714e-13	5.672e-13	5.641e-13
7.94e-01	5.771e-13	5.681e-13	5.635e-13	5.602e-13
6.31e-01	5.742e-13	5.644e-13	5.596e-13	5.560e-13
5.01e-01	5.711e-13	5.605e-13	5.553e-13	5.514e-13
3.98e-01	5.677e-13	5.563e-13	5.506e-13	5.465e-13
3.16e-01	5.641e-13	5.518e-13	5.456e-13	5.411e-13
2.51e-01	5.602e-13	5.469e-13	5.402e-13	5.354e-13
2.00e-01	5.559e-13	5.416e-13	5.344e-13	5.291e-13
1.58e-01	5.513e-13	5.358e-13	5.281e-13	5.224e-13
1.26e-01	5.464e-13	5.297e-13	5.213e-13	5.152e-13
1.00e-01	5.411e-13	5.230e-13	5.140e-13	5.073e-13
7.94e-02	5.353e-13	5.158e-13	5.060e-13	4.989e-13
6.31e-02	5.291e-13	5.080e-13	4.975e-13	4.898e-13
5.01e-02	5.223e-13	4.996e-13	4.882e-13	4.799e-13
3.98e-02	5.151e-13	4.905e-13	4.782e-13	4.693e-13
3.16e-02	5.072e-13	4.807e-13	4.675e-13	4.578e-13
2.51e-02	4.988e-13	4.701e-13	4.558e-13	4.454e-13
2.00e-02	4.896e-13	4.587e-13	4.433e-13	4.320e-13
1.58e-02	4.797e-13	4.463e-13	4.297e-13	4.176e-13
1.26e-02	4.690e-13	4.329e-13	4.150e-13	4.020e-13
1.00e-02	4.575e-13	4.185e-13	3.992e-13	3.853e-13
7.94e-03	4.450e-13	4.028e-13	3.822e-13	3.673e-13
6.31e-03	4.314e-13	3.858e-13	3.638e-13	3.480e-13
5.01e-03	4.166e-13	3.673e-13	3.439e-13	3.273e-13
3.98e-03	4.005e-13	3.471e-13	3.227e-13	3.054e-13
3.16e-03	3.826e-13	3.250e-13	2.999e-13	2.824e-13
2.51e-03	3.625e-13	3.010e-13	2.758e-13	2.548e-13
2.00e-03	3.383e-13	2.753e-13	2.507e-13	2.339e-13
1.58e-03	3.048e-13	2.485e-13	2.252e-13	2.092e-13
1.26e-03	2.730e-13	2.214e-13	1.997e-13	1.848e-13
1.00e-03	2.441e-13	1.948e-13	1.747e-13	1.612e-13
7.94e-04	2.171e-13	1.688e-13	1.507e-13	1.386e-13
6.31e-04	1.879e-13	1.437e-13	1.280e-13	1.176e-13
5.01e-04	1.547e-13	1.200e-13	1.070e-13	9.830e-14
3.98e-04	1.258e-13	9.854e-14	8.809e-14	8.106e-14
3.16e-04	1.002e-13	7.970e-14	7.153e-14	6.598e-14
2.51e-04	7.901e-14	6.368e-14	5.739e-14	5.310e-14
2.00e-04	6.184e-14	5.038e-14	4.558e-14	4.229e-14
1.58e-04	4.819e-14	3.954e-14	3.588e-14	3.336e-14
1.26e-04	3.746e-14	3.081e-14	2.802e-14	2.609e-14

TABLE 5-1



z	0.0	45.0	60.0	75.0
1.00e-04	2.904e-14	2.383e-14	2.169e-14	2.023e-14
7.94e-05	2.235e-14	1.827e-14	1.665e-14	1.555e-14
6.31e-05	1.697e-14	1.385e-14	1.265e-14	1.184e-14
5.01e-05	1.259e-14	1.038e-14	9.512e-15	8.922e-15
3.98e-05	9.112e-15	7.673e-15	7.072e-15	6.658e-15
3.16e-05	6.520e-15	5.607e-15	5.202e-15	4.920e-15
2.51e-05	4.632e-15	4.057e-15	3.791e-15	3.603e-15
2.00e-05	3.274e-15	2.912e-15	2.739e-15	2.616e-15
1.58e-05	2.304e-15	2.076e-15	1.966e-15	1.886e-15
1.26e-05	1.616e-15	1.472e-15	1.402e-15	1.351e-15
1.00e-05	1.130e-15	1.039e-15	9.947e-16	9.622e-16
7.94e-06	7.882e-16	7.310e-16	7.027e-16	6.821e-16
6.31e-06	5.485e-16	5.125e-16	4.945e-16	4.815e-16
5.01e-06	3.809e-16	3.582e-16	3.469e-16	3.386e-16
3.98e-06	2.641e-16	2.498e-16	2.426e-16	2.374e-16
3.16e-06	1.828e-16	1.738e-16	1.693e-16	1.660e-16
2.51e-06	1.264e-16	1.207e-16	1.178e-16	1.157e-16
2.00e-06	8.725e-17	8.365e-17	8.185e-17	8.053e-17
1.58e-06	6.016e-17	5.789e-17	5.676e-17	5.593e-17
1.26e-06	4.145e-17	4.001e-17	3.930e-17	3.877e-17
1.00e-06	2.853e-17	2.762e-17	2.717e-17	2.684e-17
7.94e-07	1.962e-17	1.905e-17	1.876e-17	1.855e-17
6.31e-07	1.348e-17	1.312e-17	1.294e-17	1.281e-17
5.01e-07	9.256e-18	9.029e-18	8.915e-18	8.832e-18
3.98e-07	6.352e-18	6.208e-18	6.137e-18	6.084e-18
3.16e-07	4.356e-18	4.266e-18	4.221e-18	4.188e-18
2.51e-07	2.986e-18	2.929e-18	2.900e-18	2.880e-18
2.00e-07	2.046e-18	2.010e-18	1.992e-18	1.979e-18
1.58e-07	1.401e-18	1.378e-18	1.367e-18	1.359e-18
1.26e-07	9.591e-19	9.448e-19	9.376e-19	9.324e-19
1.00e-07	6.563e-19	6.473e-19	6.428e-19	6.395e-19
7.94e-08	4.490e-19	4.433e-19	4.404e-19	4.383e-19
6.31e-08	3.070e-19	3.034e-19	3.016e-19	3.003e-19
5.01e-08	2.099e-19	2.076e-19	2.065e-19	2.057e-19
3.98e-08	1.435e-19	1.420e-19	1.413e-19	1.408e-19
3.16e-08	9.803e-20	9.712e-20	9.667e-20	9.634e-20
2.51e-08	6.697e-20	6.640e-20	6.611e-20	6.590e-20
2.00e-08	4.574e-20	4.538e-20	4.520e-20	4.507e-20
1.58e-08	3.123e-20	3.101e-20	3.089e-20	3.081e-20
1.26e-08	2.133e-20	2.118e-20	2.111e-20	2.106e-20

TABLE 5-1 (CONTINUED)



z	0.0	45.0	60.0	75.0
1.00e-08	1.456e-20	1.447e-20	1.442e-20	1.439e-20
7.94e-09	9.936e-21	9.879e-21	9.851e-21	9.830e-21
6.31e-09	6.781e-21	6.745e-21	6.727e-21	6.714e-21
5.01e-09	4.627e-21	4.604e-21	4.593e-21	4.585e-21
3.98e-09	3.157e-21	3.143e-21	3.135e-21	3.130e-21
3.16e-09	2.154e-21	2.145e-21	2.140e-21	2.137e-21
2.51e-09	1.469e-21	1.463e-21	1.461e-21	1.458e-21
2.00e-09	1.002e-21	9.984e-22	9.966e-22	9.953e-22
1.58e-09	6.834e-22	6.811e-22	6.800e-22	6.792e-22
1.26e-09	4.661e-22	4.646e-22	4.639e-22	4.634e-22
1.00e-09	3.178e-22	3.169e-22	3.165e-22	3.161e-22
7.94e-10	2.167e-22	2.161e-22	2.158e-22	2.156e-22
6.31e-10	1.478e-22	1.474e-22	1.472e-22	1.471e-22
5.01e-10	1.007e-22	1.005e-22	1.004e-22	1.003e-22
3.98e-10	6.868e-23	6.853e-23	6.846e-23	6.841e-23
3.16e-10	4.682e-23	4.673e-23	4.668e-23	4.665e-23
2.51e-10	3.191e-23	3.186e-23	3.183e-23	3.181e-23
2.00e-10	2.175e-23	2.172e-23	2.170e-23	2.169e-23
1.58e-10	1.483e-23	1.481e-23	1.479e-23	1.479e-23
1.26e-10	1.011e-23	1.009e-23	1.009e-23	1.008e-23
1.00e-10	6.889e-24	6.880e-24	6.875e-24	6.875e-24

TABLE 5-1 (CONTINUED)



$$H_{\phi}(1,50\mu\text{rad}) = (3.664 \times 10^{-14}) \text{ k}^2 \text{ rad}^2 \quad (5.1)$$

Using  $\lambda = .55 \times 10^{-6} \text{ m}$  in equation (5.1) gives:

$$H_{\phi}(1,50\mu\text{rad}) = 4.78 \text{ rad}^2 \quad (5.2)$$

This is obviously a significant error. It corresponds to an rms error of approximately  $.35\lambda$  which is about 3.5 times greater than the total wavefront error typically budgeted for all error sources in an optical system. It is this unacceptably large anisoplanatic phase error which generates the requirement for the separation between the reference beacon and the receiver.

## 5.2 Reduction of the Anisoplanatic Error Through Use of the Optimum Linear Estimate

Before evaluating the error in the estimate we must stop to realize that equations (4.30) and (4.31) only provide the optimum estimate for the selected observed data set  $\{g_i(\vec{\rho})\}$ . The equations do not tell us how to select the elements of the set. We will thus evaluate the performance of the estimation procedure for different numbers of elements in the set and for different angular spacings. We will compare the error for each of the optimum estimates to select which elements should be chosen for inclusion in  $\{g_i(\vec{\rho})\}$ .

First we use equation (4.31) to find  $\vec{a}$  for each  $\{g_i(\vec{\rho})\}$ , then we find the mean square error using:

$$\langle e^2 \rangle = \langle [g(\vec{\rho}, \vec{\psi} + \vec{\theta}) - \hat{g}(\vec{\rho}, \vec{\psi} + \vec{\theta})]^2 \rangle \quad (5.3)$$



Before we can solve equation (4.31) we must evaluate the  $F_\phi$ 's.

In appendix A we show that:

$$F_\phi(\vec{\rho}, \vec{\theta}) = (2.91/2) k^2 \rho^{5/3} (\sec \psi) [2I_2 - I_1] \quad (5.4)$$

where:  $I_1$  is the integral in equation (4.24); and

$$I_2 = \int_0^\infty C_n^2(h) dh \quad (5.5)$$

To determine the performance of the estimation procedure as a function of the look back angle,  $\theta_L$ , where:

$$\theta_L = n(\psi_i - \psi_{i+1}) \quad (5.6)$$

we choose  $n = 2$ ,  $\rho = 1$  m,  $\psi = \alpha = 0$ , and let:

$$0.05 < (\theta_L/\theta) < 1 \quad (5.7)$$

for values of  $\theta$  between 5 and 50  $\mu$ rad. In figure 5-2 we plot the reduction in mean square error achieved by the estimate as a function of the ratio of  $\theta_L$  to  $\theta$ . From figure 5-2 we see that the performance of the estimate is not a strong function of this ratio.

In figure 5-3 we plot the maximum reduction in mean square error, for  $n = 2$ , for each point ahead angle of figure 5-2. The estimate is seen to give reasonable performance (i.e., 20% improvement) for point ahead angles less than 8  $\mu$ rad, while providing very marginal performance for a point ahead angle of 50  $\mu$ rad.



PERFORMANCE OF THE OPTIMUM LINEAR ESTIMATE FOR  $n = 2$

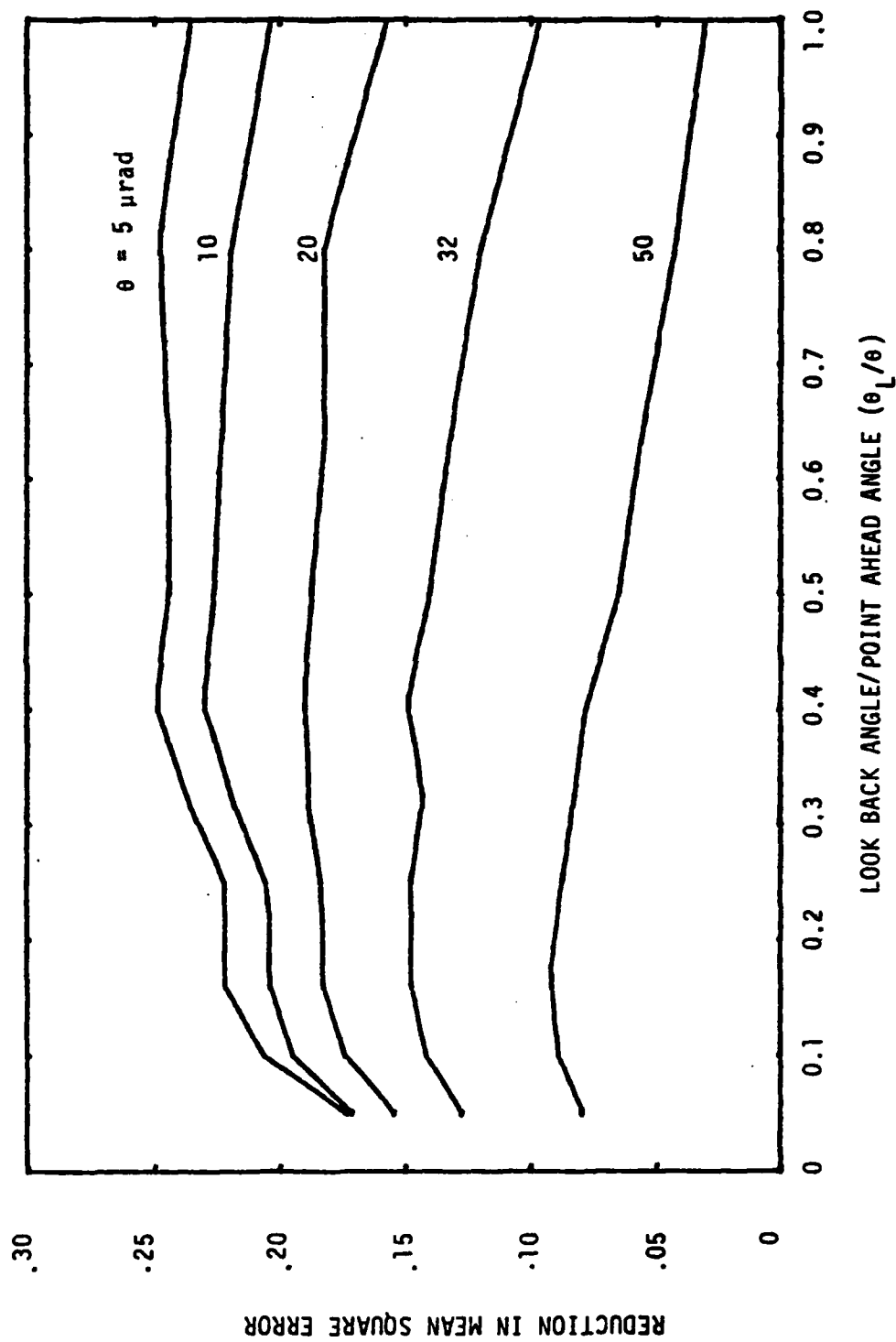


FIGURE 5-2



PERFORMANCE OF THE OPTIMUM LINEAR ESTIMATE FOR  $n = 2$

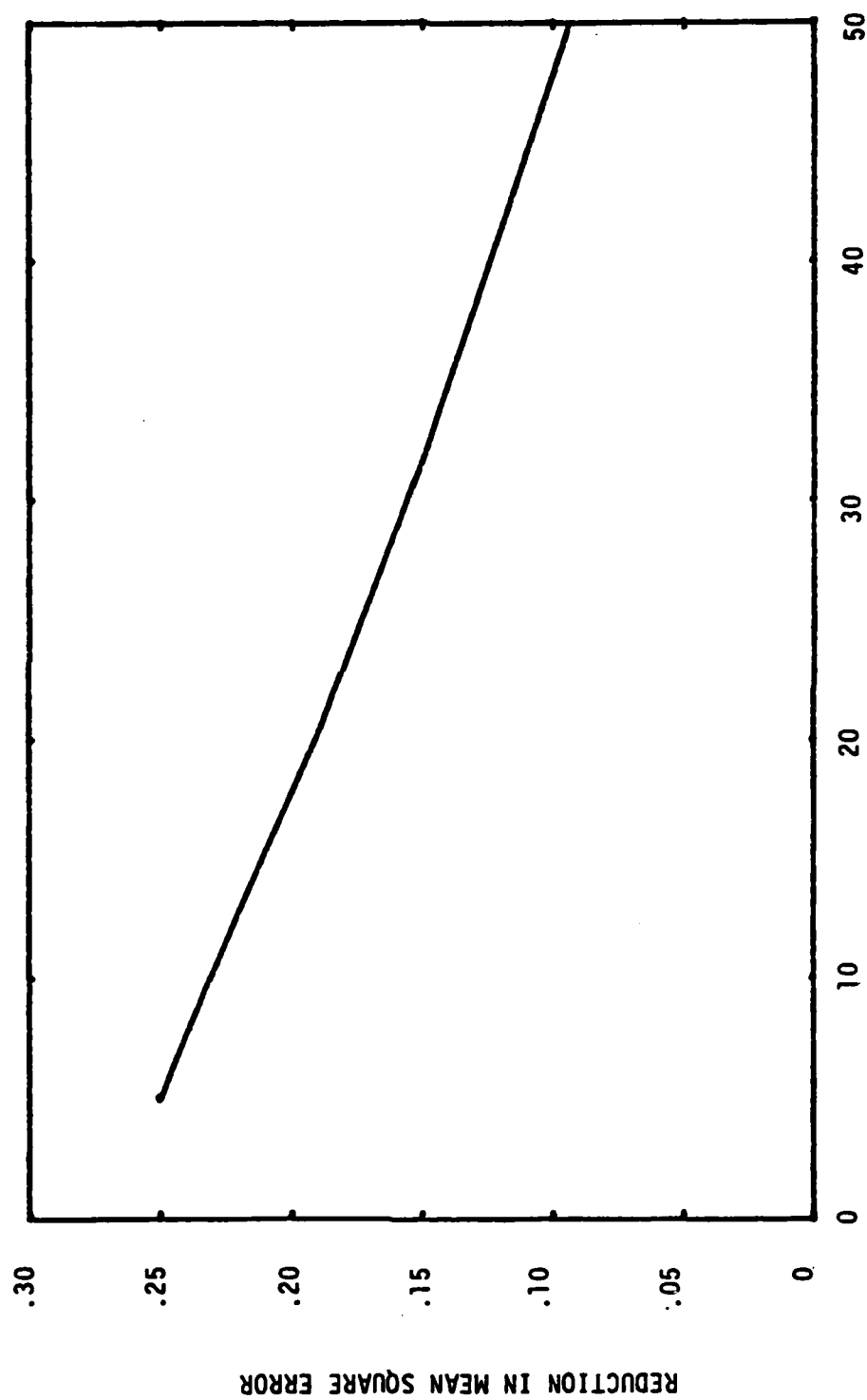


FIGURE 5-3



To determine how the performance of the estimate varies with  $n$  we duplicate the calculations made for figure 5-2 except we let  $n = 3$ . The results of these calculations are shown in figure 5-4. Comparing figures 5-2 and 5-4 we see that little improvement is gained by increasing the number of data points in the estimate from two to three. The performance of the estimate for an  $n$  of four was calculated for three cases. Also performance of a single point estimate, i.e.,  $n = 1$  was calculated. The mean square error for all cases is given in table 5-2. As can be seen from this table the single point estimate provides no improvement.

Figure 5-5 shows the relationship between the reduction in mean square error and the number of data points in the estimate. Clearly there is no value in using an  $n$  of four, and only very slight gain in performance in going from an  $n$  of two to an  $n$  of three.



PERFORMANCE OF THE OPTIMUM ESTIMATE FOR  $n = 3$

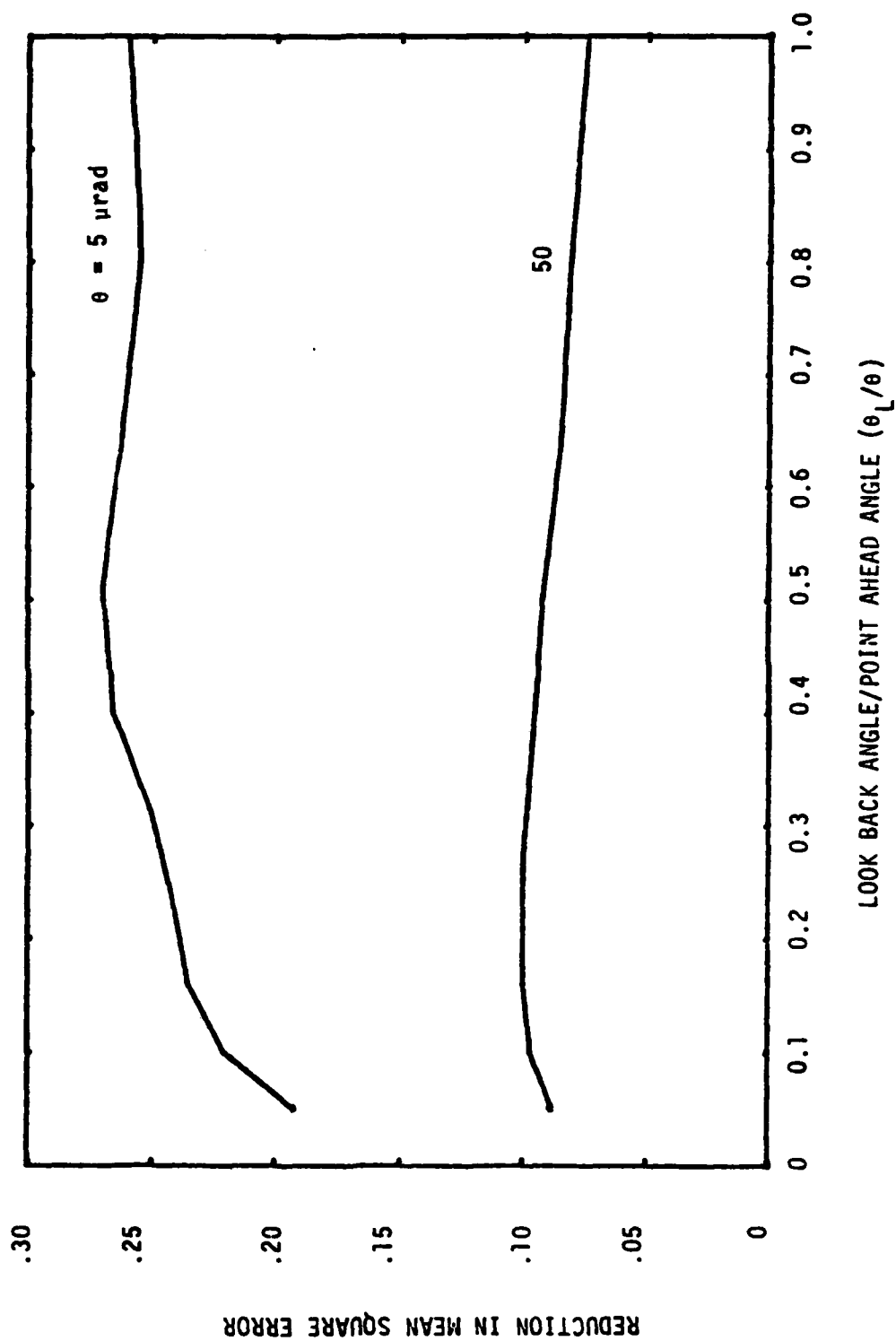


FIGURE 5-4



TABLE 5-2

MEAN SQUARE ERROR IN RAD<sup>2</sup> AT  $\lambda = .55 \mu\text{m}$   
POINT AHEAD ANGLE IN  $\mu\text{RAD}$

n	5	10	20	32	50
0	0.145	0.429	1.243	2.476	4.781
1	0.145	0.429	1.242	2.470	4.759
2	0.109	0.331	1.007	2.108	4.342
3	0.106				4.303
4	0.107				4.303



PERFORMANCE OF THE OPTIMUM LINEAR ESTIMATE

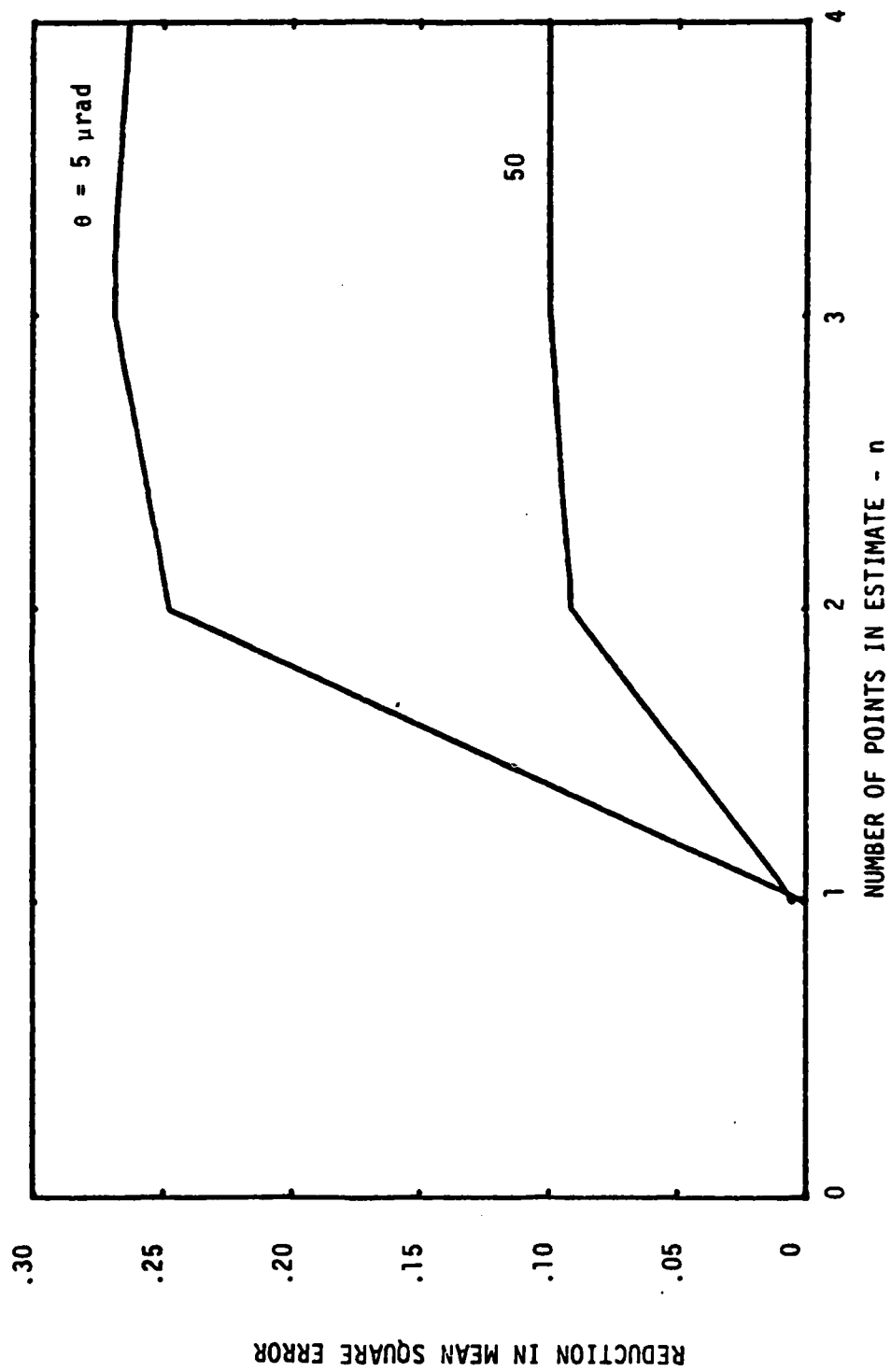


FIGURE 5-5



## VI CONCLUSIONS

### 6.1 Discussion of Results

The data in figure 5-5 shows clearly that there is little value in using more than two data points in the estimate. We believe that the basic reason for this is that the linear component of phase distortion (i.e., wavefront tilt) is the major contributor to the atmospherically induced wavefront aberrations<sup>29</sup>. Therefore, the major contributor to the anisoplanatic error is the difference in the tilt of the two wavefronts arriving from different angles. Thus, once a good estimate is made of the linear portion of the anisoplanatic error, little is gained by adding estimates of the higher order aberrations. The data in figures 5-2 and 5-4 show that the performance of the estimate is not a strong function of the look back angle. We believe that this is also a result of the fact the phase aberrations are mostly linear, and that a good estimate of this component can be made over a wide range of look back angles. One would also expect that the estimate would provide better results for small point ahead angles, as shown in figure 5-3, since for small angles there is better correlation between the measured data and the desired data than there is for larger angles. We believe that the magnitude of the improvement shown in figure 5-2 is significant as discussed in the next section.



## 6.2 System Implications

To establish a reasonable station keeping specification we can interpret the point ahead angle in figure 5-2 to be the station keeping error allowable between the beacon and the desired receiver. From table 5-2 we see that the mean square wavefront error for a station keeping error of a  $5 \mu\text{rad}$  is  $.145 \text{ rad}^2$ , at a wavelength of  $.5 \mu\text{m}$ . This corresponds to an rms wavefront error of  $.06\lambda$ , which is a reasonable budget for the station keeping error, since an optical system with a  $.1\lambda$  rms wavefront error is considered a good system. Through utilization of the estimation process developed in this paper the allowable station keeping error can be increased by approximately 15% while maintaining the same wavefront error. Although this increase seems small, it is truly significant since it could extend the lifetime of a system costing 100's of millions of dollars, for a very nominal investment in signal processing electronics. Alternatively the weight of the propellant required to maintain the station keeping could be reduced by 15%. Since almost all space systems have difficulty meeting the design goals for system weight, use of the developed estimation procedure could make the difference between whether or not the desired system weight goals are met. Different systems may require varying station keeping requirements. In general, the more stringent the station keeping specification, the more the benefit from the estimation procedure developed herein.



It is important to point out that the data needed to obtain this optimum linear estimate, i.e., the  $F_\phi$ 's in equation (4.31), are already available in current adaptive optical systems. No a priori knowledge of the turbulence profile, or any other atmospheric characteristics, is required.

### 6.3 Recommendations for Future Work

It is hoped that the results of this work will stimulate others to investigate the anisoplanatic problem. The use of techniques developed for acoustic imaging<sup>30</sup> could possibly be applied to the anisoplanatic problem. We also believe that the developed estimation procedures could be usefully applied to many real world problems where the correlation function is not well behaved.



# APPENDIX A

## SIMPLIFICATION OF THE HYPERSTRUCTURE FUNCTION

To solve equation (4.31) we need to evaluate  $F_\phi(\vec{\rho}, \vec{\theta})$  and  $F_\phi(\vec{\rho}, 0)$ . As noted in section 2.3:

$$F_\phi(\vec{\rho}, 0) = D_\phi(\rho) \quad (\text{A.1})$$

Since Kolmogorov turbulence is assumed we can use equation (4.6) to determine  $D_\phi(\rho)$ . The simplification of  $F_\phi(\vec{\rho}, \vec{\theta})$  is not as straight forward.

From equation (4.21) we have:

$$F_\phi(\vec{\rho}, \vec{\theta}) = 8.16 k^2 (4\pi^2)^{-1} \int_0^L dv C_n^2(v) I(v) \quad (\text{A.2})$$

where:

$$I(v) = \int d\vec{\sigma} \sigma^{-11/3} \{ [1 - \exp(i\vec{\sigma} \cdot \vec{\rho})] [\cos(\vec{\sigma} \cdot \vec{\theta} v) + \cos(v\sigma^2/k)] \} \quad (\text{A.3})$$

Using:

$$\cos x = [\exp(ix) + \exp(-ix)]/2$$

in equation (A.3) gives:

$$I(v) = \int d\vec{\sigma} \sigma^{-11/3} \{ (1/2) \exp[i(\vec{\sigma} \cdot \vec{\theta} v)] + (1/2) \exp[-i(\vec{\sigma} \cdot \vec{\theta} v)] \} \quad (\text{A.4})$$

$$\begin{aligned} & - (1/2) \exp[i\vec{\sigma} \cdot (\vec{\rho} + \vec{\theta} v)] - (1/2) \exp[i\vec{\sigma} \cdot (\vec{\rho} - \vec{\theta} v)] \\ & + [1 - \exp(i\vec{\sigma} \cdot \vec{\rho})] \cos[(v\sigma^2)/2] \} \end{aligned} \quad (\text{A.5})$$



Using<sup>22</sup>:

$$\int d\vec{\sigma} f(\sigma) \exp(i\vec{\sigma} \cdot \vec{\rho}) = 2\pi \int_0^{\infty} d\sigma \sigma f(\sigma) J_0(\sigma\rho) \quad (\text{A.6})$$

where:  $J_0$  is the well known Bessel function of the first kind, of order zero;

in equation (A.5) gives:

$$\begin{aligned} I(v) = 2\pi \int_0^{\infty} d\sigma \sigma^{-8/3} \{ & (1/2) J_0(\sigma\theta v) + (1/2) J_0(-\sigma\theta v) \\ & - (1/2) J_0(\sigma|\vec{\rho} + \vec{\theta}v|) - (1/2) J_0(\sigma|\vec{\rho} - \vec{\theta}v|) \\ & + [1 - J_0(\sigma\rho)] [\cos(v\sigma^2/k)] \} \end{aligned} \quad (\text{A.7})$$

Using the law of cosines we get:

$$|\vec{\rho} + \vec{\theta}v| = [\rho^2 - 2\rho\theta v \cos\alpha + (\theta v)^2] \quad (\text{A.8})$$

where:  $\alpha$  is the angle between  $\vec{\rho}$  and  $\vec{\theta}$

Using equation (A.8) in equation (A.7) gives:

$$\begin{aligned} I(v) = 2\pi \int_0^{\infty} d\sigma \sigma^{-8/3} \{ & J_0(\sigma\theta v) - (1/2) J_0[\sigma(\rho^2 - 2\rho\theta v \cos\alpha + \theta^2 v^2)^{1/2}] \\ & - (1/2) J_0[\sigma(\rho^2 + 2\rho\theta v \cos\alpha + \theta^2 v^2)^{1/2}] \\ & + [1 - J_0(\theta\rho)] [\cos(v\sigma^2/k)] \} \end{aligned} \quad (\text{A.9})$$

Adding and subtracting 1 in equation (A.9) to the quantity in curly brackets and using<sup>18</sup>:

$$\begin{aligned} \int_0^{\infty} t^{-\mu} [1 - J_0(t)] dt = & \{\Gamma[(\mu-1)/2]\} \{\Gamma[(3-\mu)/2]\} \\ & \{2^{-\mu}\} \{\Gamma[(\mu+1)/2]\}^{-2} \end{aligned} \quad (\text{A.10})$$

allows us to evaluate the first three terms of the integral.



We get:

$$\begin{aligned}
 I(v) = & 2\pi \{ -[\Gamma(5/6)][\Gamma(1/6)](2^{-8/3})[\Gamma(11/6)]^{-2} [(\theta v)^{5/3} \\
 & - (1/2) (\rho^2 - 2\rho\theta v \cos\alpha + \theta^2 v^2)^{5/6} \\
 & - (1/2) (\rho^2 + 2\rho\theta v \cos\alpha + \theta^2 v^2)^{5/6} \} \\
 & + \int_0^\infty d\sigma \sigma^{-8/3} [1 - J_0(\sigma\rho)] \cos[(v\sigma^2/k)] \} \quad (A.11)
 \end{aligned}$$

Using<sup>18</sup>:

$$x[\Gamma(x)] = \Gamma(x+1) \quad (A.12)$$

in equation (A.11) gives:

$$\begin{aligned}
 I(v) = & 2\pi \{ (-6/5) (2^{-8/3}) [\Gamma(1/6)][\Gamma(11/6)]^{-1} [(\theta v)^{5/3} \\
 & - (1/2) (\rho^2 - 2\rho\theta v \cos\alpha + \theta^2 v^2)^{5/6} \\
 & - (1/2) (\rho^2 + 2\rho\theta v \cos\alpha + \theta^2 v^2)^{5/6} \} \\
 & + I^- \} \quad (A.13)
 \end{aligned}$$

where:

$$I^- = \int_0^\infty d\sigma \sigma^{-8/3} [1 - J_0(\sigma\rho)] \cos[(v\sigma^2)/k] \quad (A.14)$$

Using equations (4.8) and (A.13) in equation (A.2) gives:

$$\begin{aligned}
 F_\phi(\vec{\rho}, \vec{\theta}) = & (-2.91/2) k^2 \int_0^L dv C_n^2(v) \{ (\theta v)^{5/3} \\
 & - (1/2) [\rho^2 - 2\rho\theta v (\cos\alpha) + (\theta v)^2]^{5/6} \\
 & - (1/2) [\rho^2 + 2\rho\theta v (\cos\alpha) + (\theta v)^2]^{5/6} \} \\
 & + (8.16/2\pi) k^2 \int_0^L dv C_n^2(v) I^- \quad (A.15)
 \end{aligned}$$



Letting  $\theta = 0$  and using equation (A.1) in equation (A.15) gives:

$$D_{\phi}(\rho) = (2.91/2)\rho^{5/3}k^2 \int_0^L dv C_n^2(v) + (8.16/2\pi)k^2 \int_0^L dv C_n^2(v) I^- \quad (A.16)$$

Using equation (4.8) in equation (A.16) gives:

$$(8.16/2\pi) \int_0^L dv C_n^2(v) I^- = (2.91/2) \rho^{5/3} \int_0^L dv C_n^2(v) \quad (A.17)$$

Using equation (A.17) in equation (A.15) gives:

$$\begin{aligned} F_{\phi}(\vec{\rho}, \vec{\theta}) = & (2.91/2)k^2 \int_0^L dv C_n^2(v) \{ \rho^{5/3} - [(\theta v)^{5/3} \\ & - (1/2) [\rho^2 - 2\rho\theta v(\cos\alpha) + (\theta v)^2]^{5/6} \\ & - (1/2) [\rho^2 + 2\rho\theta v(\cos\alpha) + (\theta v)^2]^{5/6} \} \end{aligned} \quad (A.18)$$

Letting:  $v = h \sec\psi$ ; and (A.19)

$z = (\theta \sec\psi)/\rho$ ; where (A.20)

$\psi = \text{zenith angle}$

in equation (A.18) gives:

$$\begin{aligned} F_{\phi}(\vec{\rho}, \vec{\theta}) = & (2.91/2)\rho^{5/3} [\sec(\psi)] k^2 \\ & \{ 2 \int_0^{\infty} [C_n^2(h) dh] - I_1(z, \alpha) \} \end{aligned} \quad (A.21)$$

where:

$$\begin{aligned} I_1(z, \alpha) = & \int_0^{\infty} dh C_n^2(h) \{ 1 + (zh)^{5/3} - (1/2) [1 - 2zh(\cos\alpha) \\ & + (zh)^2]^{5/6} - (1/2) [1 + 2zh(\cos\alpha) + (zh)^2]^{5/6} \} \end{aligned} \quad (A.22)$$



Equation (A.21) is the desired end result of this appendix. In general, equation (A.21) must be evaluated numerically for a specific turbulence profile of interest. Values for  $I_1$ , for a specific profile are given in table 5-1.



## REFERENCES

1. Sir Isaac Newton, Opticks, Book I, Part I, Prop VIII, Prob II (1730) (republished by Dover, New York, 1952).
2. J.W. Hardy, "Active Optics: A New Technology for the Control of Light," Proc. IEEE 66, 651 (1978).
3. R.F. Lutomirski and H.T. Yura, "Propagation of a Finite Optical Beam in an Inhomogeneous Medium," Applied Optics 10, 1652 (1971).
4. J.W. Goodman, Introduction to Fourier Optics, (McGraw-Hill Book Company, Inc., New York, 1968).
5. A.N. Kolmogorov, "The Local Structure of Turbulence in Incompressible Viscous Fluid for Very Large Reynolds' Numbers," Doklady Akad. Nauk SSSR, 30, 301 (1941).
6. V.I. Tatarski, Wave Propagation in a Turbulent Medium, (McGraw-Hill Book Company, Inc., New York, 1961).
7. D.L. Fried, "Theoretical Study of Non-Standard Imaging Concepts," RADC-TR-74-185, (May 1974).
8. R.S. Lawrence and J.W. Strohbehn, "A Survey of Clear-Air Propagation Effects Relevant to Optical Communications," Proc. IEEE 58 1523 (1970).
9. D.L. Fried, "Optical Heterodyne Detection of an Atmospherically Distorted Wave Front," Proc. IEEE 55, 57 (1967).
10. D.L. Fried, "Optical Resolution Through a Randomly Inhomogeneous Medium for Very Long and Very Short Exposures," J. Opt. Soc. Am. 56, 1372 (1966).
11. D.W. Hanson, "Temperature Turbulence Measurements at AMOS," AGARD Conference Proceedings 238, 44-1 (1978).
12. M.I. Skolnik, Radar Systems (McGraw-Hill Book Company, Inc., New York 1962), p. 262.
13. J.F. Doyle, "Compensated Imaging System Design and Performance Analysis," RADC-TR-77-69 Volume II, (March 1977).
14. C.R. Guiliano, "Non-linear Adaptive Optics," AGARD Proceedings on Special Topics in Optical Propagation, to be published.



15. A Papoulis, Probability, Random Variables and Stochastic Processes, (McGraw-Hill Book Company, Inc., New York, 1965).
16. H.L. Van Trees, Detection, Estimation, and Modulation Theory, Part I, (John Wiley and Sons, Inc., New York, 1968).
17. J.W. Strohbehn, Laser Beam Propagation in the Atmosphere, (Springer-Verlag, Berlin, 1978).
18. M. Abramowitz and I.A. Stegun, Handbook of Mathematical Functions, (Dover Publications, Inc., New York, 1965).
19. R.E. Hufnagel, "Variations of Atmospheric Turbulence," OSA Topical Meeting on Optical Propagation Through the Atmosphere, paper WA1, (July 1974).
20. D.L. Fried, "Theoretical Study of Non-Standard Imaging Concepts," RADC-TR-74-276, 4, (October 1974).
21. J.H. Shapiro, "Point Ahead Limitation on Reciprocity Tracking," J. Opt. Soc. Am. 65, 65 (1975).
22. D.L. Fried, "Spectral and Angular Covariance of Scintillation for Propagation in a Randomly Inhomogeneous Medium," Applied Optics 10 721 (1971).
23. J.W. Strohbehn, "Line-of-Sight Wave Propagation Through the Turbulent Atmosphere," Proc. IEEE 56 1301 (1968).
24. D.P. Greenwood and D.L. Fried, "Power Spectra Requirements for Wave-Front Compensative Systems," J. Opt. Soc. Am. 66 193-206 (1976).
25. G.I. Taylor, "The Spectrum of Turbulence," Proc. Roy. Soc. London A132, 476-490 (1938).
26. S.L. Valley, Handbook of Geophysics and Space Environments, (Air Force Cambridge Research Laboratories, 1965), p. 4-24.
27. M. Miller and P. Zieske, "Turbulence Environment Characterization," RADC-TR-79-131, 31 (July 1979).
28. D.L. Fried, "Isoplanatism Dependence of a Ground-To-Space Laser Transmitter With Adaptive Optics," Optical Sciences Company Report TR-249 (March 1977).
29. D.L. Fried, "Statistics of a Geometric Representation of Wavefront Distortion," J. Opt. Soc. Am. 55, 1427 (1965).
30. K.Y. Wang, "Special Issue on Acoustic Imaging," Proc. IEEE 67 (1979).



